Accepted Manuscript

Discovery of coumarin-dihydroquinazolinone analogs as niacin receptor 1 agonist with *in-vivo* anti-obesity efficacy

L. Ravithej Singh, Ajeet Kumar, Akanksha Upadhyay, Sampa Gupta, Gopala Reddy Palanati, Kamakshi Sikka, Mohammad Imran Siddiqi, Prem N. Yadav, Koneni V. Sashidhara

PII: S0223-5234(18)30371-4

DOI: 10.1016/j.ejmech.2018.04.037

Reference: EJMECH 10386

To appear in: *European Journal of Medicinal Chemistry*

Received Date: 20 February 2018

Revised Date: 5 April 2018

Accepted Date: 18 April 2018

Please cite this article as: L.R. Singh, A. Kumar, A. Upadhyay, S. Gupta, G.R. Palanati, K. Sikka, M.I. Siddiqi, P.N. Yadav, K.V. Sashidhara, Discovery of coumarin-dihydroquinazolinone analogs as niacin receptor 1 agonist with *in-vivo* anti-obesity efficacy, *European Journal of Medicinal Chemistry* (2018), doi: 10.1016/j.ejmech.2018.04.037.

Graphical Abstract

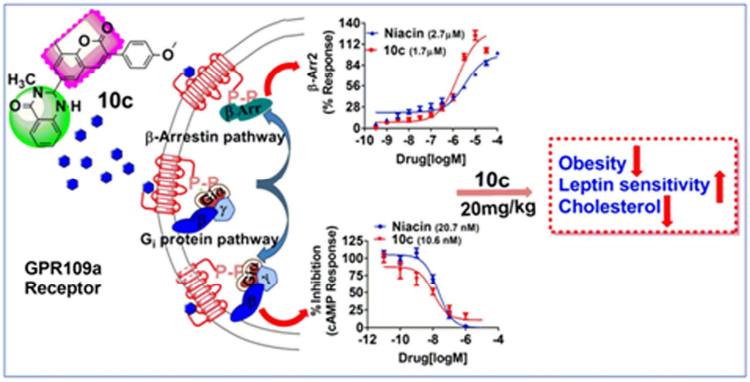

Discovery of coumarin-dihydroquinazolinone analogs as niacin receptor 1 agonist with *in-vivo* anti-obesity efficacy

L. Ravithej Singh[‡#], Ajeet Kumar[§#], Akanksha Upadhyay[‡], Sampa Gupta[‡], Gopala Reddy Palanati[‡], Kamakshi Sikka[†], Mohammad Imran Siddiqi[†], Prem N. Yadav[§,*], Koneni V. Sashidhara[‡,*]

[‡]*Medicinal and Process Chemistry Division,* [§]*Pharmacology Division,* [†]*Molecular and Structural Biology Division, CSIR-Central Drug Research Institute, BS-10/1, Sector 10, Jankipuram extension, Sitapur Road, Lucknow 226031, India.*

[#] These authors contributed equally

Keywords:

Niacin, niacin receptor 1, GPR109a, pharmacophore hybridization, coumarin-dihydroquinazolinone, Homology modeling

***Corresponding authors.**

Tel.: +91 9919317940; Fax: +91-522-2628493.

Email: kv_sashidhara@cdri.res.in, sashidhar123@gmail.com (Dr. K. V. Sashidhara), pn.yadav@cdri.res.in (Dr. P. N. Yadav)

Graphical abstract

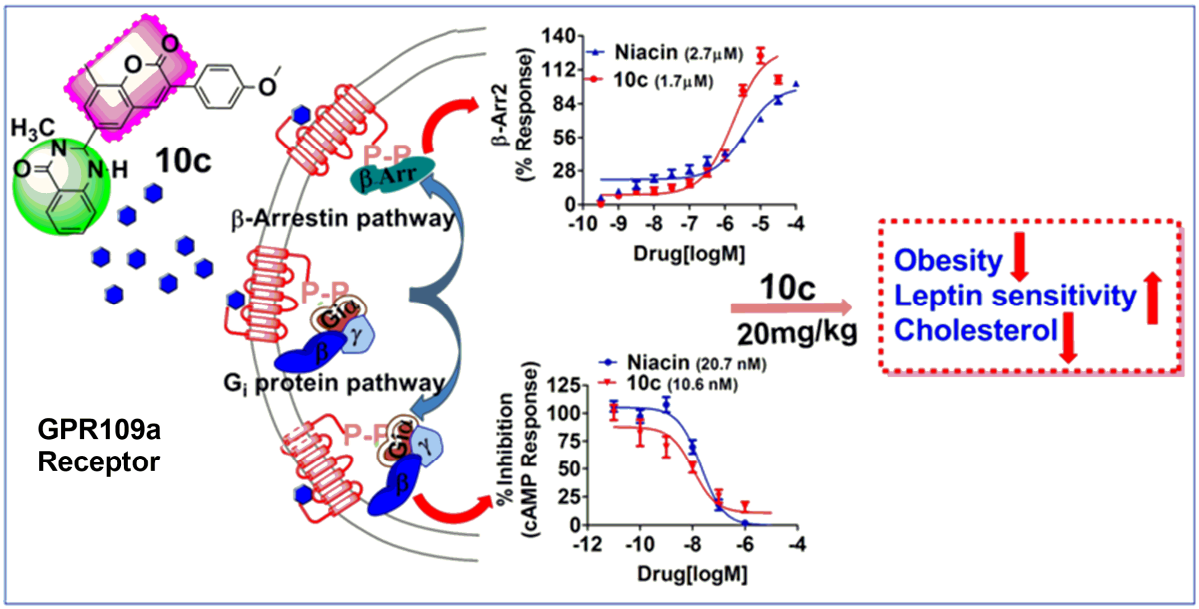

Abstract:

In this study, we presented rational designing and synthesis of coumarin-dihydroquinazolinone conjugates to evaluate their agonist activity at GPR109a receptor. Among the synthesized small molecule library, compound **10c** displayed robust agonist action at GPR109a with EC_{50}< 11nM. Homology model of human GPR109a protein was generated to realize the binding interaction of the active molecule with the active site of GPR109a. Further, the efficacy of active compound **10c** was supported by *in-vivo* experiments which showed reduced body weight in diet induced obese mice model. Interestingly, compound **10c** reduced leptin in blood plasma and total serum cholesterol. These results suggest that the coumarin-dihydroquinazolinone conjugate is a suitable scaffold to further expand the chemical diversity and make them potential niacin receptor 1 agonist.

1. Introduction

Nicotinic acid (NA), also known as niacin or vitamin B-3, is a well-known lipid modifying agent in humans [1]. NA therapy has been shown to produce several beneficial effects, such as reducing the major coronary events by 25%, stroke by 26%, and all cardiovascular events by 27% [2]. Moreover, NA has also been shown to quite effective for lowering triglycerides and LDL cholesterol, raising HDL level in blood [3]. Multiple lines of evidence confirmed that the G protein-coupled receptor GPR109a is a molecular target of NA [4-6]. GPR109a, also known as hydroxy-carboxylic acid 2 (HCA2) receptor or niacin receptor 1(NIACR1), is highly expressed in adipocytes, spleen and immune cells such as macrophage, keratinocytes and Langerhans cells and mediates the lipid-lowering effect of NA [5]. Rahman M *et al.* reported that GPR109a is also expressed in brain microglia and exhibited neuroprotective effect in mice [7]. However, NA mediated activation of GPR109a in langerhans cells and keratinocytes induces expression of prostaglandin D2 (PGD2) and ultimately cutaneous flushing [8, 9] by β-arrestin1 mediated signaling [10]. Thus, a G-protein bias agonist of GPR109a that exhibits minimal or no β-arrestin1 dependent signaling would be a better candidate to avoid the side effect of targeting GPR109a. Therefore, there are renewed interests to synthesize G-protein biased agonist of GPR109a.

Although NA has been shown to inhibit lipolysis through activation of the GPR109a in adipose tissues [5], one study provided quite strong evidence that the NA effects on blood lipid profile are independent of the GPR109a [11]. Besides, these studies also demonstrated the effects of NA via GPR109a expressed in adipose tissue increased plasma level of adiponectin and anti-inflammatory cytokine expression in obesity [12, 13]. Expressions of GPR109a have been shown to increase during differentiation of adipocytes from preadipocytes as well as after activation of

peroxisome proliferator-activated receptor-gamma (PPARγ) [14]. Thus, it is quite clear that GPR109a modulates pleiotropic effects besides well known therapeutic effects on lipid metabolism [15]. Therefore, search for new ligands that bind to GPR109a to accomplish desired effects by subtracting or minimizing adverse effects has gained momentum. Medicinal chemistry efforts from academia and industries towards the development of potent GPR109a agonist resulted in the discovery of several novel small molecules. For example, pyridopyrimidinone and *aza*-pyridopyrimidinone derivatives (**1** and **2**, Figure 1) were identified as GPR109a agonists [16]. Similarly, Merck research laboratory discovered pyrano[2,3-*d*]pyrimidine (**3**, Figure 1) class of compound processing nicotinic acid receptor agonist activity for dyslipidemia with *in-vivo* efficacy [17].

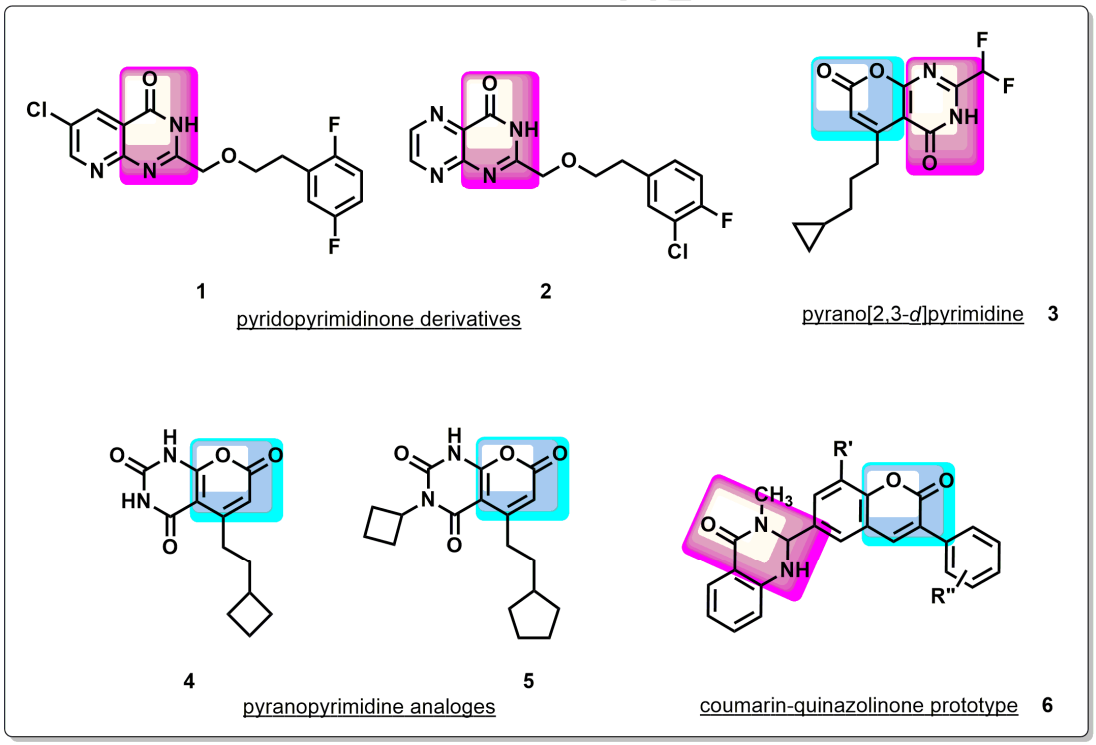

Fig. 1. Chemical structures with potent GPR109a agonist activity and general structure of our synthesized prototype

Interestingly, a distinct fused heterocyclic motif, pyranopyrimidine (**4** and **5**, Figure 1), comprising barbituric acid and pyrone ring exhibited promising activity in a cell-based cAMP assay, which is also a GPR109a agonist [18]. In the quest for new drug leads, the hybridization approach has been a promising one, which involves the combination of pharmacophoric moieties to produce a hybrid structure with improved efficacy and reduced toxicity. The derivatives of coumarin are well known pharmacophores with potential benefits in the prevention of obesity and liver dysfunction [19]. Also, we have reported the utility of coumarin analogs as good lipid-lowering agents [20]. On the other hand, quinazolinone and its derivatives are the vital constituents of number of natural products and modern drugs [21-23]. Quinazolinone and its derivatives exhibit a wide range of biological activities including antitumor, antiviral, anti-inflammatory, analgesic, antifungal, antimalarial, antidiabetic, anticonvulsant, antimicrobial, and angiotensin II AT_1 receptor antagonists [24-31]. Inspired by wide and interesting biological activity of Quinazolinone scaffold, we synthesized the novel coumarin- dihydroquinazolinone hybrids (**6**, Figure 1), and evaluated for their G-protein and arrestin biased agonist activity at GPR109a receptors.

2. Results and Discussion:

2.1 Chemistry

The synthesis of target compounds (**10a-10p**) is shown in Scheme 1. The first step involved a reaction of commercially available 2-alkyl phenols (**7a-7g**) with hexamethylenetetramine (HMTA) in trifluoroacetic acid at 110°C [32]. The resulting dialdehyde compounds (**8a-8g**) were then treated with substituted phenylacetic acids in the presence of cyanuric chloride, and N-methyl morpholine (NMM) in DMF at 110°C conditions promoted the desired 3-aryl coumarins (**9a-9p**) [33]. Further which were engaged in multicomponent reaction with methylamine and

isatoic anhydride in acetic acid resulted in the formation of final target coumarin-dihydroquinazolinone conjugates (**10a-10p**) in good yields.

To study the role of aryl coumarin, we made structural diversity on the 2, 3-dihydroquinazolinone scaffold, the key 2-hydroxy-3-methyl-5-(3-methyl-4-oxo-1, 2, 3, 4-tetrahydroquinazolin-2-yl) benzaldehyde (**11**) intermediate was obtained from the multicomponent reaction of isatoic anhydride, methylamine and 5-methyl-4-hydroxyisophthalaldehyde (**8a**) in acetic acid [34]. Access to the coumarin-dihydroquinazolinone

Scheme 1: Synthesis of coumarin-dihydroquinazolinone conjugates (**10a-10p)**.

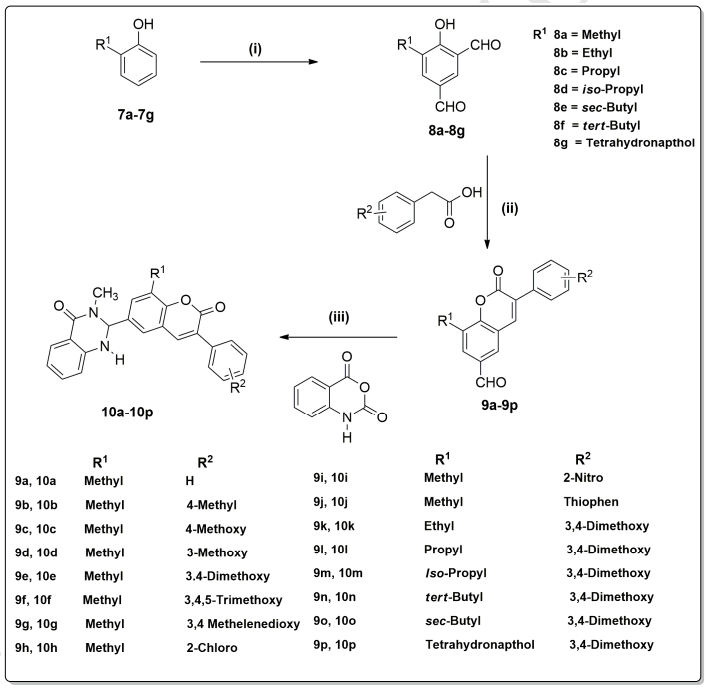

	R^1	R^2		R^1	R^2
9a, 10a	Methyl	H	9i, 10i	Methyl	2-Nitro
9b, 10b	Methyl	4-Methyl	9j, 10j	Methyl	Thiophen
9c, 10c	Methyl	4-Methoxy	9k, 10k	Ethyl	3,4-Dimethoxy
9d, 10d	Methyl	3-Methoxy	9l, 10l	Propyl	3,4-Dimethoxy
9e, 10e	Methyl	3.4-Dimethoxy	9m, 10m	*Iso*-Propyl	3,4-Dimethoxy
9f, 10f	Methyl	3,4,5-Trimethoxy	9n, 10n	*tert*-Butyl	3,4-Dimethoxy
9g, 10g	Methyl	3,4 Methelenedioxy	9o, 10o	*sec*-Butyl	3,4-Dimethoxy
9h, 10h	Methyl	2-Chloro	9p, 10p	Tetrahydronapthol	3,4-Dimethoxy

Reagents and conditions: (i) a. HMTA / TFA, 120 ºC, 3.0 h; b. 10% H_2SO_4, 90-100 ºC, 2.0 h; (ii) Cyanuric chloride, NMM, DMF, 110 ºC, 30-90 min.; (iii) Methyl amine, acetic acid, 110 ºC, 1.0-2.0 h

ester derivatives (**12a** and **12b**) were achieved upon treatment of intermediate **11**, with malonic esters in ethanol catalyzed by piperidine [35]. Benzofuran-dihydroquinazolinones (**13a** and **13b**) were obtained by treatment of **11** with phenacyl bromide derivatives in acetonitrile and K_2CO_3 as

a base under reflux conditions [36]. Furthermore, enamines-dihydroquinazolinone (**14a** and **14b**) were obtained by the reaction of **11** and aniline derivatives in ethanol [37]. The complete reaction conditions and reagents are illustrated in Scheme 2. The structures of all the synthesized intermediates and targeted compounds were supported by the spectral ^{1}H NMR and ^{13}C NMR data, the results of mass spectrometry which were in agreement with the proposed structures. The purity of the tested compounds was found to be >95% by HPLC analysis.

Scheme 2: Structural diversity on the 2, 3 dihydroquinazolinone scaffolds (11)

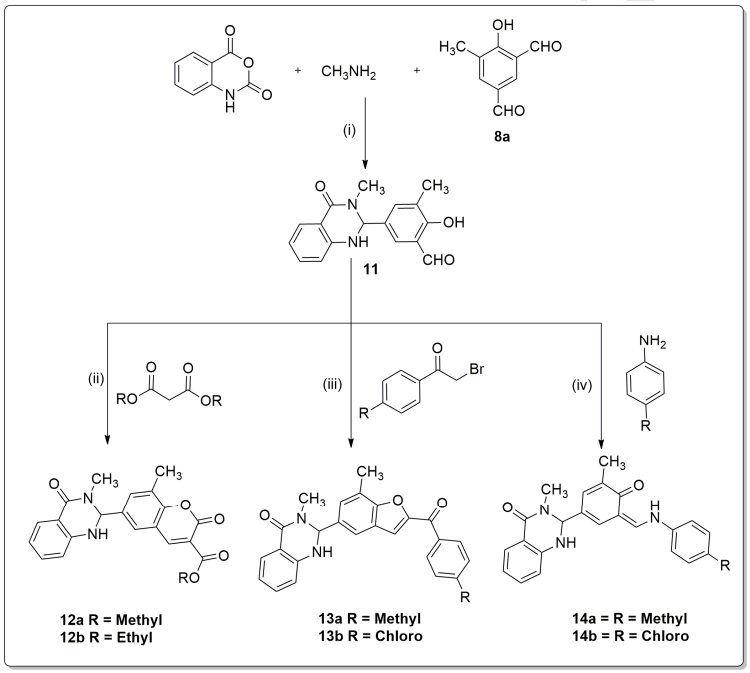

Reagents and conditions: (i) AcOH, 110 ºC, 2.0h; (ii) Piperidine, ethanol, 80 ºC, 1.0 h; (iii) K_2CO_3, CH_3CN, reflux, 4.0 h; (iv) Ethanol, rt, 15 min.

2.2. Pharmacology

2.2.1 Cell-based high throughput screening for GPR109a biased agonist

First, we evaluated twenty-two coumarin-dihydroquinazolinone (10a-10p, 12a, 12b, 13a, 13b, 14a and 14b) analogs for agonist activity at GPR109a receptor using GloSensor assay that

measures cAMP in live cells according to previously used method with some modification [38]. We observed that the compound **10b** and **10c** showed cAMP inhibition in a dose-dependent manner (EC_{50} 30.5 nM & 10.6 nM Fig-2A & Table 1), while NA, which was used as reference agonist exhibited EC_{50} 20.7 nM. Compound **10c** showed slightly better affinity than NA with EC_{50} < 11 nM vs 20.7 nM (Fig- 2A). However, compound **10g**, **10j** & **10k** were modestly active and inhibited cAMP formation at 10µM concentration (Table 1).

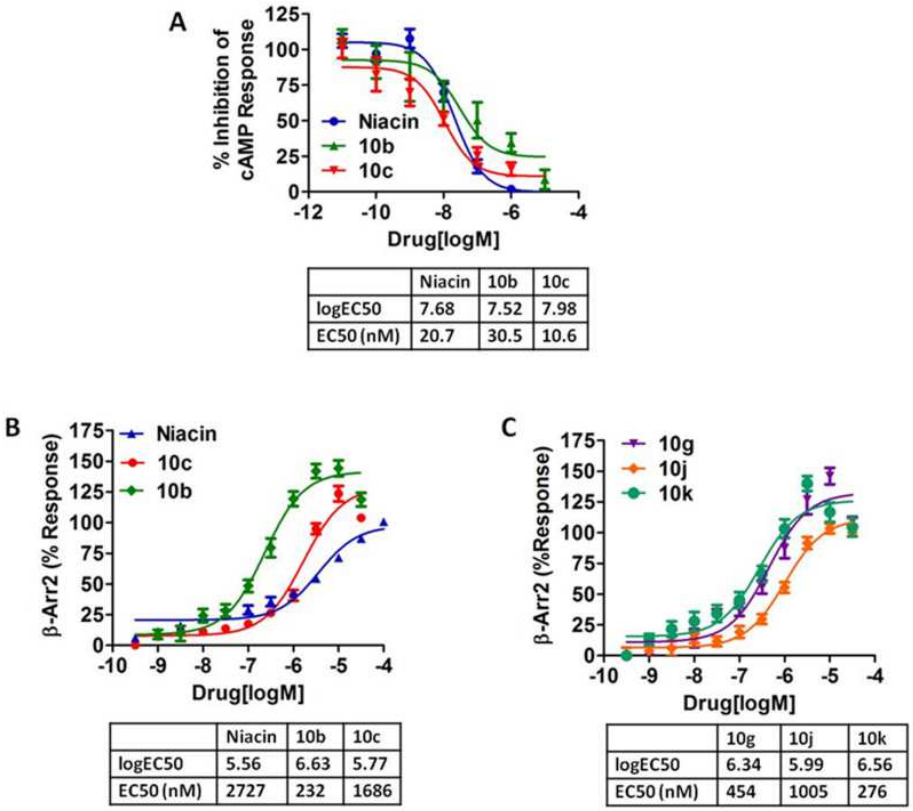

	Niacin	10b	10c
logEC50	7.68	7.52	7.98
EC50 (nM)	20.7	30.5	10.6

	Niacin	10b	10c
logEC50	5.56	6.63	5.77
EC50 (nM)	2727	232	1686

	10g	10j	10k
logEC50	6.34	5.99	6.56
EC50 (nM)	454	1005	276

Fig. 2. Representative dose-response curve of GPR109a mediated cAMP inhibition and β-arrestin recruitment: Concentration response curve of **10b**, **10c** with niacin (reference ligand) at GPR109a for agonist activity in transiently transfected HEK293T cells by using cAMP GloSensor assay (**A**). Similarly, concentration dependent curve of **10b**, **10c** and niacin (**B**) and **10g**, **10j** and **10k** (**C**) for recruitment of β-arrestin was assessed in

transiently transfected HTLA cells. Data are expressed as mean ± S.E.M. of normalized results of three individual experiments.

To determine the β-arrestin dependent signaling of these compounds, we examined five active compounds in the β-arrestin-Tango assay. Following 12 h of treatment with **10b**, **10c**, **10g**, **10j**, **10k** and NA as a reference compound, we found that all the tested compounds show a dose-dependent increase in β-arrestin recruitment (Fig 2b & 2c). we observed that all compounds have micromolar range affinity and are close to NA in the β-arrestin-Tango assay (Table 1). *In vitro* data suggests that **10c** has slightly more potency than NA in Gi-protein dependent GPR109a signaling (GloSensor assay), but have quite a similar effect in β-arrestin dependent GPR109a signaling (arrestin-tango assay).

Table 1: Functional selectivity of Niacin, 10c and its derivatives at GPR109a receptor

	Compounds	EC_{50} in GloSensor Assay	EC_{50} in Tango Assay
1	Niacin	**20.7 nM** (pEC_{50}=7.683±0.09)	**2727 nM** (pEC_{50}=5.56±0.07)
2	**10b**	**30.5 nM** (pEC_{50}=7.516±0.38)	**232 nM** (pEC_{50}=6.63±0.07)
3	**10c**	**10.6 nM** (pEC_{50}=7.975±0.18)	**1686 nM** (pEC_{50}=5.77±0.06)
4	**10g**[#]	≥10 µM	**454 nM** (pEC_{50}=6.34±0.09)
5	**10j**[#]	≥10 µM	**1005 nM** (pEC_{50}=5.99±0.08)
6	**10k**[#]	≥10 µM	**276 nM** (pEC_{50}=6.56±0.10)

[#]These compounds did not show dose dependent activity (active only at 10µM concentration) in GloSensor assay.

2.2.2 Structure activity relationship

A series of coumarin-dihydroquinazolinone analogs were synthesized and screened for agonist activity on GPR109a. Our aim was to determine if coumarin-dihydroquinazolinone analogs exhibit G-protein bias or β–arrestin bias agonist activity at GPR109a. Preliminary analysis reveals that compound having mono substitution at *para* position of phenyl ring with strong

electron donating group (EDG) such as methoxy (**10c**) showed greater affinity towards G-protein dependent pathway (pEC_{50}=7.98) compared to β-arrestin dependent pathway (pEC_{50}= 5.77). Furthermore, compound with weak EDG such as methyl derivative (**10b)** displayed slightly low affinity (pEC_{50}=7.52) for the G-protein dependent pathway, while increased affinity for β-arrestin dependent pathway (pEC_{50}=6.6). The substitutions at both *meta* and *para* position with methelendioxy (**10g)** or dimethoxy (**10k)** was not tolerated ($pEC_{50} \geq 5$) in G- protein dependent pathway but no change was observed in affinity (pEC_{50}=6.0 to 6.6) in β-arrestin dependent pathway. Interestingly, heteroaromatic substitution of phenyl ring for example thiophenyl ring (**10j),** exhibited persistent β-arrestin dependent activity (pEC_{50}=5.99), but decrease in G-protein dependent activity ($pEC_{50} \geq 5$).

2.2.3 Docking studies

Homology models were built due to the non-availability of the crystal structure of *Homo sapiens* GPR109a and processed for validation study using PDBsum Generate tool [47]. Out of 10 models, a model was selected whose most of the residues (93.8%) lie in the favored region of Ramachandran Plot created by PROCHECK, whereas 4.7%, 1.6%, 0.0% residues occur in the additional allowed region, generously allowed region and disallowed region respectively (Fig 3a). The selected model shows a root mean square deviation (RMSD) of 0.43Aº on superimposition with the template (Fig 3b). In order to get insight into the binding mode of (R) and (S) isomers in the racemic mixture of the compound **10c**, docking study was performed.

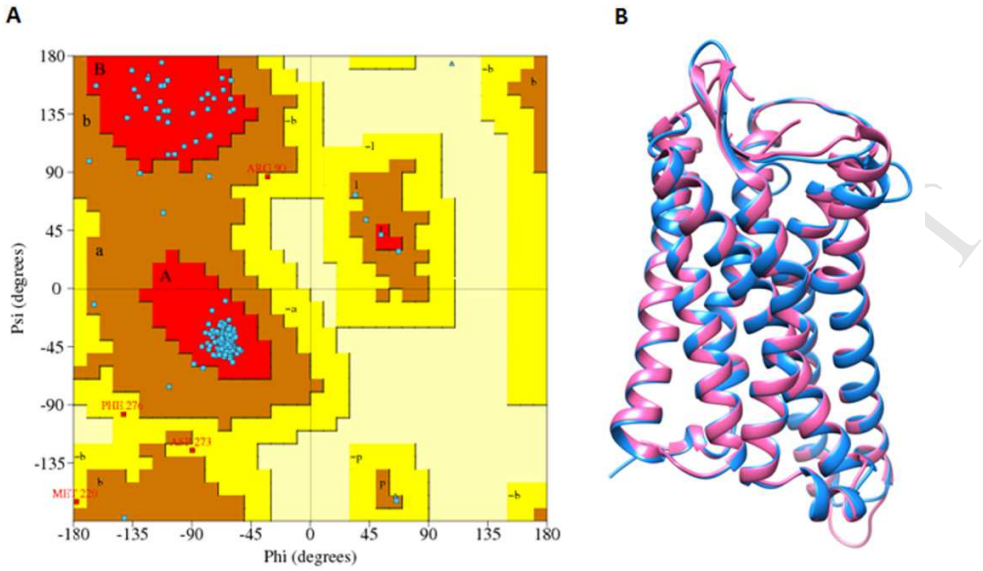

Fig 3: **(A)** Ramachandran plot of GPR109a modeled protein. The different colored areas indicate "disallowed" (light yellow), "generously allowed" (yellow), "additional allowed" (brown), and "most favored" (red) regions.
(B) Superimposed structures of GPR109a homology modeled (*blue*) and template of active μ-opioid receptor bound to an agonist selected as a template (*PDB identifier: 5C1M pink*)

GPR109a has a well-characterised agonist binding pocket with residues surrounding mainly from transmembrane (TM) and extracellular (EC) regions [48]. Based on the previous studies [49, 50], Asn86 (EC1), Trp91 (EC1), Arg111 (TM3), Asn171 (EC2), Ser178 (EC2), Ser179 (EC2), Ser247 (TM6), Arg251 (EC3), Ile254 (EC3), Phe255 (EC3), His259 (EC3), Try283 (TM7), Tyr284 (TM7), residues were selected for docking study. Those docked conformations were chosen which show interaction with key binding site residues with the suitable binding pose. Both (R) and (S) isomers fit well into the binding cavity of the protein and showed relatively similar molecular interaction with the surrounding residues. (R)-isomer of the compound **10c** docked into the trans-membrane binding pocket has formed a cluster of 15 poses with the lowest binding energy of -8.87 kcal/mol and manifestation of strong molecular interaction is in the form of hydrogen bonds with Arg111 at 2.039Aº and Tyr284 at 2.14Aº (Fig 4a). Further inspection of

the docked structure has also revealed the presence of non-bonded T-shaped π-π interaction with Phe276 and hydrophobic interactions with Leu34, Leu83, Leu107, and Leu280. In the case of (S)-isomer, a cluster of 26 poses was selected based on the lowest binding energy of -9.49 kcal/mol. Apart from hydrogen bond interaction with Arg111 and Tyr284, (S)-isomer also formed a hydrogen bond with the backbone of Cys177 (Fig 4b). Along with T-shaped π-π interaction with Phe276, π-cation interaction was also observed with Arg111. Various hydrophobic interactions with residues Leu83, Trp91, Leu107, Arg111, Leu176, Cys177, Phe277, Leu280 were also observed. Consequently, we further examined the *in-vivo* anti-dyslipidemic and antiobesity effect of compound **10c** in high-fat diet induced obese mice.

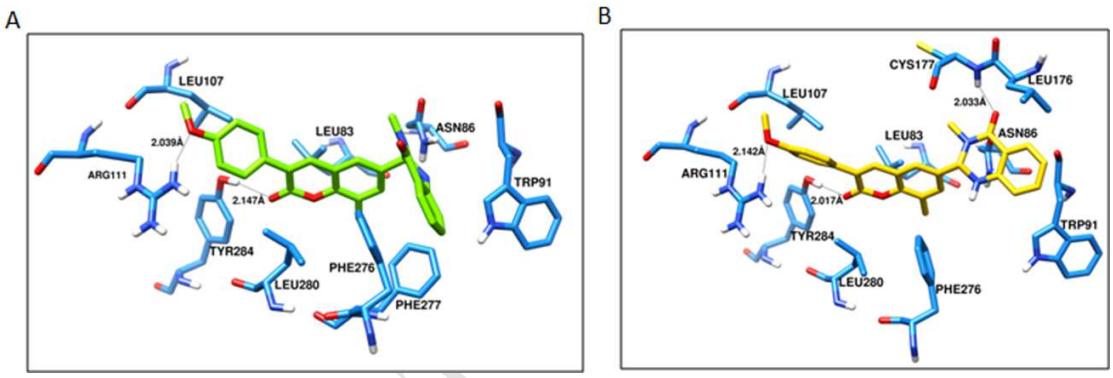

Fig. 4a. Interaction of (R)-isomer (A) and (S)-isomer (B) of compound **10c** with the GPR109a model protein.

*2.2.4 Beneficial effect of compound **10c** on obese mice*

It has been previously reported that GPR109a have the benignant effect on obesity [12, 13, 51]. Therefore we examined the anti-obesity effect of chronic (six weeks) oral administration of compound **10c** (20 mg/kg body weight) in high-fat diet (HFD) induced obese mice. Interestingly, compound **10c** significantly reduced cumulative body weight gain starting at day 20 of treatment, which was even better than reference anti-obesity drug lorcaserin (Figure 5a; n=4-5; *P< 0.05,.**P< 0.01,.***P< 0.001; Two-Way ANOVA). Finally, at the end of the experiment, we

found a significant decrease in net body weight of compound **10c** treated mice compared to HFD vehicle-treated mice (Table 2; n=6-5; p<0.0356, t-test). Consistent with the reduced body weight, mice treated with compound **10c** also had modest but not significant reduced body fat mass as compared to control mice (Fig. **5b** and Table. 2; n=4-5, P< 0.0002; One-Way ANOVA). In compound, **10c** treated obese mice did not show any significant reduction in lean weight compared to vehicle-treated mice (Table 2; n=4-5; p<0.0865, One-Way ANOVA).

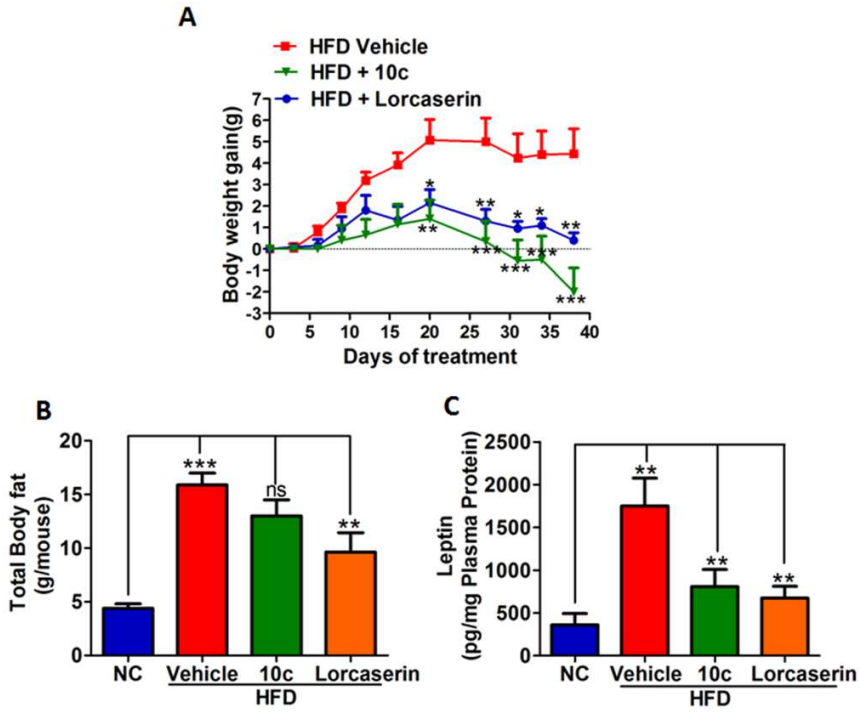

Fig. 5. Anti-obesity effect, after six weeks chronic treatment of GPR109a agonist 10c and lorcaserin (LRC) in high-fat diet (HFD) induced obese mice: HFD induced obese mice were treated with lorcaserin (10mg/kg; p.o.) or **10c** (20mg/kg; p.o.) significantly decreased body weight gain compare to vehicle-treated HFD mice *P< 0.05,.**P< 0.01,.***P< 0.001 Two-Way ANOVA. (**a**). Lorcaserin treatment significantly decreased total body fat compared to vehicle-treated HFD mice, but we did not observe the significant effect in total body fat of compound **10c** treated mice P< 0.001 One Way ANOVA followed by Newman-Keuls Multiple Comparison Test. **(b).** Compound **10c** and LRC treated obese mice significantly decreased the blood plasma level of leptin compared to vehicle-treated HFD mice P< 0.001 One-Way ANOVA followed by Newman-Keuls Multiple Comparison Test. **(c**) Data represented as. mean ± SEM of 4-5 mice/ group.

2.2.5. Chronic treatment of compound ***10c*** *decreased obesity-induced blood plasma leptin level in obese mice*

Since obesity is typically associated with high leptin levels due to the insensitivity of leptin [52], we evaluated if compound **10c** treatment modulates blood plasma level in obese mice. Interestingly, chronic treatment with compound **10c** significantly decreased blood plasma leptin level in diet-induced obese (DIO) mice (Fig 5c & Table2; P< 0.001 One-Way ANOVA). These observations suggest that treatment with active compound attenuated leptin resistance in DIO mice. Although we found no difference in glucose tolerance (Fig. 6a), we noticed significant difference in fasting blood glucose level in **10c** treated mice (Table 2, n=4-6; p<0.0273 t-test).

2.2.6 Effect of compound ***10c*** *on lipid profile in DIO mice*

Given the well established antilipolytic effect of NA [53], we measured the effect of compound **10c** on the level of various types of lipids. We found that significant decrease in total serum cholesterol in compound **10c** treated mice as compared to vehicle-treated obese mice (Fig. 6b, n=4-5; P< 0.05; t-test). However, we did not observe any significant effect of this compound on triglycerides, high-density lipoprotein (HDL) cholesterol and low-density lipoprotein (LDL) cholesterol levels in serum of DIO mice.

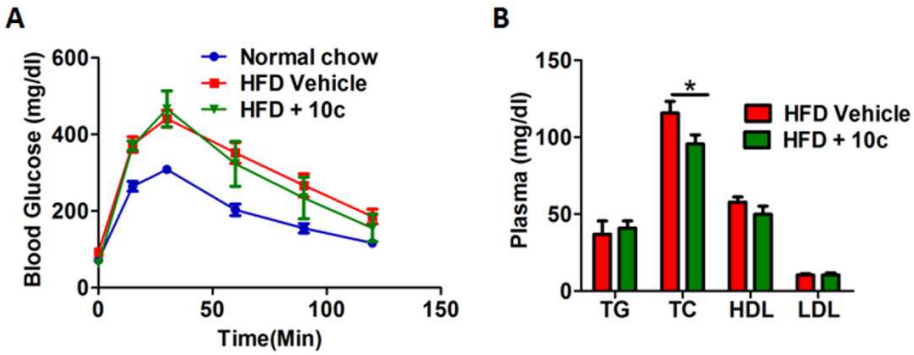

Fig. 6. Chronic treatment of GPR109a agonist have no effect in glucose tolerance test but significantly decreased total blood plasma cholesterol in obese mice: We did not observe any effect on the intraperitoneal glucose tolerance test (IPGTT) in compound **10c** treated mice**.** IPGTT was performed in 16 hours fasted mice, after the glucose administration (2g/kg body weight, *i.p*.) blood glucose level was measured at different time points 15' 30' 60' 90' and 120 minutes **(a).** Chronic treatment of compound **10c** significantly decreased total blood cholesterol level compared to vehicle-treated mice, but we did not observe any effects in triglycerides, HDLc and LDLc level of blood serum of compound **10c** treated obese mice P< 0.05;t-test **(b).** Data represented as. mean ± SEM of 4-5 mice/ group.

Table 2: Summary of measured parameters in obese mice treated with 10c or Vehicle

S. No.	Parameters	HFD Vehicle	HFD+10c	p-value	n
1	Net Body weight Change	3.867±1.108	-0.72±1.54	**0.0356**	5-6
2	Fat mass [g/mouse]	16.52 ± 1.154	13.01 ± 1.476	0.0551	4-5
3	Lean mass [g/mouse]	25.58 ± 0.6789	23.16 ± 0.664	0.0865	5-6
4	Fasting glucose [mg/dl]	93.17 ± 5.793	63.00 ± 10.80	**0.0273**	4-6
5	Plasma leptin [pg/mg protein]	1751 ± 325.4	807.6 ± 199.2	**0.0360**	4-5
6	TG [mg/dl]	40.96 ± 4.592	36.97 ± 8.558	0.7080	5-6
7	Total cholesterol [mg/dl]	120.8 ± 7.206	95.60 ± 6.007	**0.0302**	4-5
8	HDL-c [mg/dl]	57.80 ± 3.385	45.92±5.727	0.0956	5-6
9	LDL-c [mg/dl]	11.56±1.587	10.40±0.867	0.5178	5-6

3. Conclusion

In conclusion, coumarin-dihydroquinazolinone conjugates (**10a**-**10p**) have been synthesized and tested for their agonist and antagonist activity towards GPR109a receptor. The compound **10c** found to have cAMP inhibition at 10nM concentration and modulates β-arrestin dependent signaling. Subsequently, compound **10c** exhibited beneficial effects such as reduction in cumulative body weight gain and net body weight. It is evident from the blood plasma analysis

that compound **10c** decreased leptin level in plasma and reduced total serum cholesterol levels; In order to explore the role of 3-aryl coumarin, we synthesized simple 2, 3-dihydroquinazolinone, coumarin-dihydroquinazolinone ester (**12a** & **12b**), furan (**13a** & **13b**) and enamines (**14a** & **14b**), however, none of them were found to be active . Taken together, these findings highlighted the coumarin-dihydroquinazolinone conjugate as a suitable scaffold to further expand the chemical diversity and make them potential niacin receptor 1 agonist.

Experimental section:

4. Chemistry

4.1.1. General synthetic procedure for preparation of 4-hydroxy-5-alkyl isophthalaldehydes (8a-8g)

2-Alkyl phenol (1.0 mmol) and hexamethylenetetramine (1.2 mmol) were dissolved in TFA (25 mL), and the solution was heated at 120 ºC for 3.0 h. After cooling to room temperature 10 % aq.H_2SO_4 (25 mL) was added and again the temperature maintained at 90-100 ºC for two more hours. After completion, the solution was basified with Na_2CO_3 to pH 8 and extracted 3-fold with 25 mL of $CHCl_3$. The combined organic layers were dried on Na_2SO_4, filtered, and concentrated to dryness under reduced pressure. The crude product was purified on silica gel column (100-200 mesh) using 20% EtOAc/hexane as eluent to afford compounds **8a-8g** in good yields.

4.1.1. 4-hydroxy-5-methylisophthalaldehyde (8a)

White solid; Yield: 60%; m.p.: 125 - 127 ºC; IR (neat): 3262, 2865, 1703, 1626, 1013 cm^{-1}; ^1H NMR ($CDCl_3$, 300 MHz): δ 11.82 (s, 1H), 9.97 (s, 1H), 9.90 (s, 1H), 7.97 (d, *J* = 1.8 Hz, 1H), 7.93 (brs, 1H), 2.33 (s, 3H); ^{13}C NMR ($CDCl_3$, 75 MHz): δ 196.4, 189.9, 165.0, 137.2, 134.8, 128.7, 125.2, 119.7, 15.1; ESI-MS: (m/z): 164 $[M+H]^+$.

4.1.2. 5-Ethyl-4-hydroxyisophthalaldehyde (8b)

White solid, yield: 69%; mp: 173-174 °C; IR (neat, cm^{-1}): 3259, 2870, 1700, 1628, 1013; ^1H NMR ($CDCl_3$, 400 MHz): *δ* 11.85 (s, 1H), 9.98 (s, 1H), 9.91 (s, 1H), 7.97-7.95 (m, 2H), 2.78-2.72 (m, 2H), 1.26 (t, *J* = 7.5 Hz, 3H); ^{13}C NMR ($CDCl_3$, 75 MHz): δ 196.4, 189.7, 164.6, 135.4, 134.7, 134.3, 128.8, 119.7, 22.1, 13.2; ESI-MS (*m/z)*: 179 $(M+H)^+$.

4.1.3.. 4-Hydroxy-5-propylisophthalaldehyde (8c)

Oily; yield: 62%; IR (neat, cm^{-1}): 3259, 2872, 1710, 1620, 1010; ^{1}H NMR ($CDCl_3$, 400 MHz): δ 11.85 (s, 1H), 9.96 (s, 1H), 9.89 (s, 1H), 7.96 (d, *J* = 2.0 Hz, 1H), 7.91 (d, *J* = 2.0 Hz, 1H), 2.68 (t, *J* = 6.6 Hz, 2H), 1.71-1.61 (m, 2H), 0.96 (t, *J* = 7.3 Hz, 3H); ^{13}C NMR ($CDCl_3$, 100 MHz): δ 196.4, 189.7, 164.7, 136.4, 134.7, 132.8, 128.7, 119.8, 30.9, 22.1, 13.8; ESI-MS: (*m/z*): 193 $(M+H)^+$.

4.1.4.. 4-hydroxy-5-isopropylisophthalaldehyde (8d)

White solid; yield; 89%; m.p.: 164-163 ºC; IR (KBr): 3028, 1677, 1665, 1615, 1229, 768 cm^{-1}; ^{1}H NMR ($CDCl_3$, 300 MHz): δ 11.94 (s, 1H), 9.97 (s, 1H), 9.91 (s, 1H), 7.99 (brs, 1H), 7.96 (d, *J* =1.47 Hz,1H), 3.43-3.33 (m, 1H), 1.27 (d, *J* =5.1 Hz, 6H); ^{13}C NMR ($CDCl_3$, 75 MHz): δ 196.6, 189.9, 164.3, 138.9, 134.8, 133.2, 129.0, 119.9, 26.5, 22.1 ; ESI-MS: (*m/z*) 265 $[M+H]^+$.

4.1.5.. 5-sec-butyl-4-hydroxy-benzene-1,3-dicarbaldehyde (8e)

Oily; Yield: 64%; IR (neat): 3267, 2862, 1709, 1622, 1018 cm^{-1}; ^{1}H NMR ($CDCl_3$, 200 MHz): δ 11.99 (s, 1H), 10.05 (s, 1H), 9.96 (s, 1H), 8.08 (brs, 1H), 8.00 (s, 1H), 3.27-3.10 (m, 1H), 1.74-1.58 (m, 2H), 1.25 (d, *J* = 7.0 Hz, 3H), 0.87 (t, *J* = 7.3 Hz, 3H); ^{13}C NMR ($CDCl_3$, 75 MHz): δ 196.4, 189.4, 163.9, 137.1, 134.5, 133.4, 128.7, 119.6, 32.7, 28.8, 19.3, 11.5; ESI-MS (m/z): 207 $[M+H]^+$.

4.1.6. 5-tert-butyl-4-hydroxyisophthalaldehyde (8f)

Oily; Yield: 65%; IR (neat): 3252, 2865, 1703, 1626, 1013 cm^{-1}; ^{1}H NMR ($CDCl_3$, 300 MHz): δ 12.39 (s, 1H), 9.99 (s, 1H), 9.93 (s, 1H), 8.07 (brs, 1H), 7.99 (brs, 1H), 1.45 (s, 9H); ^{13}C NMR ($CDCl_3$, 75 MHz): δ 196.9, 190.0, 166.1, 140.0, 135.4, 133.9, 128.6, 120.4, 35.2, 29.1; ESI-MS: (m/z): 207 $[M+H]^+$.

4.1.7. 4-hydroxy-5, 6, 7, 8-tetrahydronaphthalene-1, 3-dicarbaldehyde (8g)

White solid; yield; 65%; m.p.: 145-147 ºC; IR (KBr): 3026, 1677, 1665, 1615, 1249, 768 cm^{-1}; ^1H NMR ($CDCl_3$, 300 MHz): δ 11.86 (s, 1H), 10.15 (s, 1H), 9.92 (s, 1H), 7.92 (s, 1H), 3.24 (d, *J* =5.2 Hz, 2H), 2.74 (d, *J* =5.1 Hz, 2H), 1.84-1.82 (m, 4H); ^{13}C NMR ($CDCl_3$, 100 MHz): δ 195.9, 190.3, 163.6, 149.3, 136.8, 127.7, 126.9, 117.3, 27.4, 22.6, 21.9, 21.1; ESI-MS: (*m/z*) 205 $[M+H]^+$.

4.2.1. 8-methyl-2-oxo-3-phenyl-2H-chromene-6-carbaldehyde (9a)

Light yellow solid; yield: 86%; m.p.: 124-126 ºC; IR (KBr): 3041, 1716, 1709, 1652, 1024 cm^{-1}; ^1H NMR ($CDCl_3$, 400 MHz): δ 10.03 (s, 1H), 7.92 (d, *J* = 4.0 Hz, 2H), 7.89 (s, 1H), 7.74 (d, *J* = 1.6 Hz, 1H), 7.72 (d, *J* = 1.3 Hz, 1H) 7.49-7.46 (m, 3H), 2.58 (s, 3H); ^{13}C NMR ($CDCl_3$, 100 MHz): δ 190.4, 159.7, 155.5, 139.4, 134.1, 132.4, 129.2, 129.1, 128.6, 128.5, 128.2, 127.3, 119.6, 15.5; ESI-MS (*m/z*): 265 $[M+H]^+$.

4.2.2. 8-methyl-2-oxo-3-(p-tolyl)-2H-chromene-6-carbaldehyde (9b)

Light yellow solid; yield: 81%; m.p.: 128-130 ºC; IR (KBr): 3044, 1721, 1715, 1644, 1019 cm^{-1}; ^1H NMR ($CDCl_3$, 300 MHz): δ 10.03 (s, 1H), 7.92 (d, *J* = 5.2 Hz, 2H), 7.86 (s, 1H), 7.64 (d, *J* = 7.4 Hz, 2H), 7.30 (d, *J* = 7.4 Hz, 2H), 2.58 (s, 3H), 2.43 (s, 3H); ^{13}C NMR ($CDCl_3$, 75 MHz): δ 190.4, 159.8, 155.5, 139.4, 138.7, 132.4, 132.3, 131.2, 129.3, 129.1, 128.3, 128.1, 127.2, 119.7, 21.3, 15.5; ESI-MS (*m/z*): 279 $[M+H]^+$.

4.2.3. 3-(4-Methoxyphenyl)-8-methyl-2-oxo-2H-chromene-6-carbaldehyde (9c)

Light yellow solid; yield: 96%; m.p.: 148-150 ºC; IR (KBr): 3033, 1725, 1705, 1639, 1021 cm^{-1}; ^1H NMR ($CDCl_3$, 300 MHz): δ 9.98 (s, 1H), 7.86 (d, *J* = 4.5 Hz, 2H), 7.79 (s, 1H), 7.67 (d, *J* = 8.9 Hz, 2H), 6.96 (d, *J* = 8.5 Hz, 2H), 3.84 (s, 3H), 2.53 (s, 3H); ^{13}C NMR ($CDCl_3$, 75 MHz): δ 190.5, 160.5, 159.9, 155.3, 137.9, 132.4, 132.3, 129.9, 128.6, 128.0, 127.2, 126.4, 119.8, 114.1, 55.4, 15.5; ESI-MS (*m/z*): 295 $[M+H]^+$.

4.2.4. 3-(3-Methoxyphenyl)-8-methyl-2-oxo-2H-chromene-6-carbaldehyde (9d)

Light yellow solid; yield: 95%; m.p.: 150-152 ºC; IR (KBr): 3025, 1716, 1707, 1645, 1016 cm^{-1}; ^{1}H NMR ($CDCl_3$, 300 MHz): δ 10.01 (s, 1H), 7.88 (d, J = 10.4 Hz, 3H), 7.40-7.35 (m, 1H), 7.28-7.26 (m, 2H), 6.99-6.95 (m, 1H), 3.86 (s, 3H), 2.56 (s, 3H); ^{13}C NMR ($CDCl_3$, 75 MHz): δ 190.6, 159.7, 155.7, 139.7, 135.5, 132.8, 132.5, 129.8, 129.1, 128.4, 127.5, 121.0, 119.7, 114.9, 114.4, 55.5, 15.7; ESI-MS (*m/z*): 294 $[M+H]^+$.

4.2.5. 3-(3,4-Dimethoxyphenyl)-8-methyl-2-oxo-2H-chromene-6-carbaldehyde (9e)

Light yellow solid; yield: 98%; m.p.: 178-180 ºC; IR (KBr): 3053, 1730, 1695, 1634, 1026 cm^{-1}; ^{1}H NMR ($CDCl_3$, 300 MHz): δ 10.01 (s, 1H), 7.90 (d, J = 7.3 Hz, 2H), 7.84 (s, 1H), 7.32-7.29 (m, 2H), 6.96 (d, J = 9.0 Hz, 1H), 3.95 (s, 3H), 3.94 (s, 3H), 2.56 (s, 3H); ^{13}C NMR ($CDCl_3$, 75 MHz): δ 190.5, 159.9, 155.4, 150.2, 148.9, 138.2, 132.5, 132.4, 128.7, 128.0, 127.3, 126.8, 121.4, 119.8, 111.8, 111.2, 56.1, 56.0, 15.5; ESI-MS (*m/z*): 325 $[M+H]^+$.

4.2.6. 8-Methyl-2-oxo-3-(3,4,5-trimethoxyphenyl)-2H-chromene-6-carbaldehyde (9f)

White solid; yield: 99%; m.p.: 196-198 ºC; IR (KBr): 3074, 1728, 1695, 1632, 1010 cm^{-1}; ^{1}H NMR ($CDCl_3$, 300 MHz): δ 10.02 (s, 1H), 7.91 (m, 2H), 7.86 (s, 1H), 6.95 (s, 2H), 3.93 (s, 6H), 3.91 (s, 3H), 2.57 (s, 3H); ^{13}C NMR ($CDCl_3$, 75 MHz): δ 190.5, 159.8, 155.5, 153.4, 139.4, 139.1, 132.8, 132.6, 129.6, 129.0, 128.2, 127.4, 119.7, 106.2, 61.0, 56.4, 15.6; ESI-MS (*m/z*): 355 $[M+H]^+$.

4.2.7. 3-(benzo[d][1,3]dioxol-5-yl)-8-methyl-2-oxo-2H-chromene-6-carbaldehyde (9g)

Yellow solid; yield: 85%; m.p.: 166-168 ºC; IR (KBr): 3067, 1723, 1671, 1617, 1030 cm^{-1}; ^{1}H NMR ($CDCl_3$, 400 MHz): δ 10.03 (s, 1H), 7.91 (bs, 2H), 7.82 (s, 1H), 7.26 (d, J = 1.5 Hz 1H), 7.23 (d, J = 7.9 Hz, 1H), 6.92 (d, J = 7.9 Hz, 1H), 6.05 (s, 2H), 2.58 (s, 3H); ^{13}C NMR ($CDCl_3$,

100 MHz): δ 190.4, 159.8, 155.3, 148.6, 147.8, 138.4, 132.4, 132.4, 128.7, 128.0, 127.3, 122.6, 119.6, 109.0, 108.4, 101.4, 15.5; ESI-MS (*m/z*): 309 $[M+H]^+$.

4.2.8. 3-(2-chlorophenyl)-8-methyl-2-oxo-2H-chromene-6-carbaldehyde (9h)

Yellow solid; yield: 81%; m.p.: 203-205 ºC; IR (KBr): 3058, 1757, 1679, 1644, 1017 cm^{-1}; ^1H NMR ($CDCl_3$, 400 MHz): δ 10.04 (s, 1H), 7.96 (s, 1H), 7.93 (s, 1H), 7.83 (s, 1H), 7.54-7.52 (m, 1H), 7.45-7.42 (m, 1H), 7.41-7.38 (m, 2H), 2.59 (s, 3H); ^{13}C NMR ($CDCl_3$, 100 MHz): δ 190.3, 158.9, 156.0, 142.3, 133.5, 133.2, 133.0, 132.4, 131.2, 130.3, 130.0, 128.4, 127.9, 127.6, 126.9, 118.9, 15.5; ESI-MS (*m/z*): 299 $[M+H]^+$.

4.2.9. 8-methyl-3-(2-nitrophenyl)-2-oxo-2H-chromene-6-carbaldehyde (9i)

White solid; yield: 94%; m.p.: 285-288 ºC; IR (KBr): 3065, 1718, 1697, 1607, 1022 cm^{-1}; ^1H NMR ($CDCl_3$, 400 MHz): δ 10.02 (s, 1H), 8.18 (d, J = 8.0 Hz, 1H), 7.94 (d, J = 4.0 Hz, 2H) 7.83 (s, 1H), 7.75 (t, J = 7.4 Hz, 1H), 7.66-7.62 (m, 1H), 7.50 (d, J = 7.4 Hz, 1H), 2.56 (s, 3H); ESI-MS (*m/z*): 310 $[M+H]^+$.

4.2.10. 8-methyl-2-oxo-3-(thiophen-2-yl)-2H-chromene-6-carbaldehyde (9j)

Brown solid; yield: 84%; m.p.: 117-119 ºC; IR (KBr): 3047, 1711, 1675, 1607, 1083 cm^{-1}; ^1H NMR ($CDCl_3$, 400 MHz): δ 10.02 (s, 1H), 8.06 (s, 1H), 7.93 (s, 1H), 7.89 (s, 1H), 7.85 (d, J = 3.0 Hz, 1H), 7.48 (d, J = 5.1 Hz, 1H), 7.16 (t, J = 4.1 Hz, 1H), 2.57 (s, 3H); ^{13}C NMR ($CDCl_3$, 100 MHz): δ 190.3, 160.0, 158.6, 154.6, 135.3, 134.9, 132.5, 132.3, 128.3, 128.0, 127.7, 127.3, 122.6, 119.3, 15.5; ESI-MS (*m/z*): 271 $[M+H]^+$.

4.2.11. 3-(3, 4-dimethoxyphenyl)-8-ethyl-2-oxo-2H-chromene-6-carbaldehyde (9k)

Light yellow solid; yield: 95%; m.p.: 160-162 ºC; IR (KBr): 3065, 1728, 1697, 1607, 1032 cm^{-1}; ^1H NMR ($CDCl_3$, 300 MHz): δ 10.04 (s, 1H), 7.92 (s, 2H), 7.85 (s, 1H), 7.33-7.28 (m, 2H), 6.97

(d, *J* = 8.0 Hz, 1H), 3.95 (s, 6H), 3.00 (q, *J* = 7.4 Hz, 2H), 1.38 (t, *J* = 7.5 Hz, 3H); ESI-MS (*m/z*): 339 $[M+H]^+$.

4.2.12. 3-(3,4-dimethoxyphenyl)-2-oxo-8-propyl-2H-chromene-6-carbaldehyde (9l)

Yellow solid; yield: 94%; m.p.: 152-154 ºC; IR (KBr): 3061, 1731, 1688, 1612, 1017 cm^{-1}; ^1H NMR ($CDCl_3$, 400 MHz): δ 10.04 (s, 1H), 7.93 (s, 1H), 7.91 (s, 1H) 7.86 (s, 1H), 7.34 (s, 1H), 7.31 (d, *J* = 2.1 Hz, 1H), 6.98 (d, *J* = 8.1 Hz, 1H), 3.97 (s, 3H), 3.96 (s, 3H), 2.95 (t, *J* = 7.4 Hz, 2H), 1.85-1.76 (m, 2H), 1.05 (t, *J* = 7.0 Hz, 3H); ^{13}C NMR ($CDCl_3$, 100 MHz): δ 190.5, 159.8, 155.0, 150.0, 148.8, 138.2, 132.4, 131.6, 128.6, 128.0, 126.7, 121.3, 119.8, 111.7, 111.1, 56.0, 55.9, 31.2, 22.7, 13.8; ESI-MS (*m/z*): 353 $[M+H]^+$.

4.2.13. 3-(3,4-dimethoxyphenyl)-8-isopropyl-2-oxo-2H-chromene-6-carbaldehyde (9m)

Yellow solid; yield: 89%; m.p.: 149-151 ºC; IR (KBr): 3067, 1727, 1681, 1611, 1027 cm^{-1}; ^1H NMR ($CDCl_3$, 300 MHz): δ 10.03 (s, 1H), 7.97 (s, 1H), 7.92 (s, 1H), 7.85 (s, 1H), 7.28 (d, *J* = 7.9 Hz, 2H), 6.98 (d, *J* = 8.0 Hz, 1H), 3.95 (s, 3H), 3.94 (s, 3H), 3.73-3.66 (m, 1H), 1.37 (d, *J* = 6.8 Hz, 6H); ESI-MS (*m/z*): 353 $[M+H]^+$.

4.2.14. 8-tert-butyl-3-(3, 4-dimethoxyphenyl)-2-oxo-2H-chromene-6-carbaldehyde (9n)

Light yellow solid; yield: 91%; m.p.: 160-162 ºC; IR (KBr): 3055, 1728, 1687, 1607, 1022 cm^{-1}; ^1H NMR ($CDCl_3$, 300 MHz): δ 10.05 (s, 1H), 8.04 (s, 1H), 7.95 (s, 1H), 7.87 (s, 1H), 7.38-7.32 (m, 2H), 6.98 (d, *J* = 8.3 Hz, 1H), 3.97 (s, 3H), 3.95 (s, 3H), 1.60 (s, 9H); ESI-MS (*m/z*): 367 $[M+H]^+$.

4.2.15. 8-sec-Butyl-3-(3, 4-dimethoxyphenyl)-2-oxo-2H-chromene-6-carbaldehyde (9o)

Light yellow solid; yield: 98%; m.p.: 140-142 ºC; IR (KBr): 3065, 1728, 1697, 1607, 1032 cm^{-1}; ^1H NMR ($CDCl_3$, 300 MHz): δ 10.04 (s, 1H), 7.93 (d, *J* = 1.6 Hz, 2H), 7.86 (s, 1H), 7.33-7.29 (m, 2H), 6.96 (d, *J* = 8.6 Hz, 1H), 3.96 (s, 3H), 3.95 (s, 3H), 3.54-3.44 (m, 1H), 1.81-1.72 (m,

2H), 1.34 (d, *J* = 7.0 Hz, 3H), 0.91 (t, *J* = 7.4 Hz, 3H); ^{13}C NMR ($CDCl_3$, 75 MHz): δ 190.8, 160.0, 154.8, 150.2, 150.0, 138.6, 136.8, 132.8, 129.2, 128.8, 128.0, 126.9, 121.4, 120.1, 111.9, 111.3, 56.2, 56.1, 33.5, 29.8, 20.6, 12.1; ESI-MS (*m/z*): 367 $[M+H]^+$.

4.2.16. 3-(3, 4-dimethoxyphenyl)-2-oxo-7, 8, 9, 10-tetrahydro-2H-benzo[h]chromene-6-carbaldehyde (9p)

Light yellow solid; yield: 95%; m.p.: 185-187 ºC; IR (KBr): 3065, 1718, 1695, 1607, 1132 cm^{-1}; ^{1}H NMR ($CDCl_3$, 300 MHz): δ 10.29 (s, 1H), 7.87 (s, 1H), 7.81 (s, 1H), 7.30-7.26 (m, 2H), 6.95 (d, *J* = 6.1 Hz, 1H), 3.95 (s, 3H), 3.93 (s, 3H), 3.29 (s, 2H), 2.99 (s, 2H), 1.89-1.87 (m, 4H); ESI-MS (*m/z*): 365 $[M+H]^+$.

4.3. Typical multicomponent synthesis of coumarin-quinoline conjugates (10a-10p)

The reaction of **9a-9p** (1.0 mmol), isatoic anhydride (1.5 mmol) and methyl amine (excess) was carried out in presence of sufficient quantity of acetic acid. The reaction mixture was subjected to refluxing conditions at about 110 °C for 1.0-2.0 h. After completion of the reaction, the reaction mixture was allowed to cool up to room temperature and then cold water was added to it. A solid was obtained which was thoroughly washed with water to remove acetic acid. The crude product thus obtained was purified by column chromatography using 5% MeOH/ DCM solvent system.

4.3.1. 3-methyl-2-(8-methyl-2-oxo-3-phenyl-2H-chromen-6-yl)-2, 3-dihydroquinazolin-4(1H)-one (10a)

White solid; Yield: 90%, m.p.: 156-158 ºC; IR (KBr): 3416, 3021, 2926, 1622, 1215 cm^{-1}; ^{1}H NMR (DMSO-d_6, 300 MHz): δ 8.25 (s, 1H), 7.73-7.66 (m, 3H), 7.52 (s, 2H), 7.44-7.42 (m, 3H), 7.32 (s, 1H), 7.23-7.18 (m, 1H) 6.69-6.64 (m, 2H), 5.91 (s, 1H), 2.89 (s, 3H), 2.39 (s, 3H); ^{13}C NMR ($CDCl_3$, 75 MHz): δ 162.9, 160.0, 151.7, 146.5, 141.1, 136.9, 134.9, 133.6, 131.3, 129.0,

128.9, 128.6, 127.9, 127.3, 125.7, 124.2, 119.4, 117.6, 114.8, 114.6, 71.9, 32.4, 15.6; HRMS (ESI) calcd for $C_{25}H_{20}N_2O_3$ $[M + H]^+$, 397.1547, found 397.1571.

4.3.2. 3-methyl-2-(8-methyl-2-oxo-3-p-tolyl-2H-chromen-6-yl)-2, 3-dihydroquinazolin-4(1H)-one ***(10b)***

White solid; yield: 85%; m.p.: 238-240 ºC; IR (KBr): 3415, 3015, 2946, 1670, 1210, 1052 cm^{-1}; ^1H NMR (DMSO-d_6, 300 MHz): δ 8.23 (s, 1H), 7.68-7.61 (m, 3H), 7.50 (s, 2H), 7.36 (d, J = 1.0 Hz, 1H), 7.26-7.18 (m, 3H), 6.69-6.63 (m, 2H), 5.91 (d, J = 1.9 Hz, 1H), 2.88 (s, 3H), 2.38 (s, 3H), 2.33 (s, 3H); ^{13}C NMR (DMSO-d_6, 100 MHz): δ 162.9, 160.1, 151.5, 146.6, 140.4, 138.6, 136.9, 133.7, 132.0, 131.1, 129.2, 128.8, 127.9, 127.2, 125.7, 124.0, 119.5, 117.6, 114.8, 114.6, 71.8, 32.5, 21.3, 15.6; HRMS (ESI) calcd for $C_{26}H_{22}N_2O_3$ $[M + H]^+$, 411.1703, found 411.1659.

4.3.3. 2- (3 -(4- methoxyphenyl) -8- methyl -2-oxo-2H –chromen -6- yl) -3- methyl- 2, 3-dihydroquinazolin -4(1H)-one (10c)

White solid; yield: 85%; m.p.: 228-230 ºC; IR (KBr):3409, 3025, 2944, 1660, 1220, 1042 cm^{-1}; ^1H NMR ($CDCl_3$, 300 MHz): δ 7.98 (d, J = 7.6 Hz, 1H), 7.67-7.64 (m, 3H), 7.36 (d, J = 11.7 Hz, 2H), 7.30-7.25 (m, 1H), 6.98 (d, J = 8.6 Hz, 2H), 6.89-6.84 (m, 1H), 6.60 (d, J = 7.9 Hz, 1H), 5.74 (s, 1H), 4.76 (s, 1H), 3.86 (s, 3H), 2.92 (s, 3H), 2.42 (s, 3H); ^{13}C NMR ($CDCl_3$, 75 MHz): δ 163.6, 160.6, 160.3, 151.8, 145.3, 138.3, 135.6, 133.7, 130.5, 129.8, 128.4, 127.8, 126.8, 126.7, 123.5, 119.5, 119.2, 115.3, 114.4, 114.0, 73.5, 55.4, 32.1, 15.6; HRMS (ESI) calcd for $C_{26}H_{22}N_2O_4$ $[M + H]^+$, 427.1652, found 427.1661.

*4.3****.4.*** ***2-(3-(3-methoxyphenyl)-8-methyl-2-oxo-2H-chromen-6-yl)-3-methyl-2, 3-dihydroquinazolin-4(1H)-one (10d)***

White solid; Yield: 86%, m.p.: 160-162 ºC; IR (KBr): 3420, 3025, 2944, 1660, 1220, 1042 cm^{-1} ; ^1H NMR ($CDCl_3$, 300 MHz): δ 7.97 (d, J = 7.7 Hz, 1H), 7.74 (s, 1H), 7.41-7.35 (m, 3H), 7.28-

7.24 (m, 3H), 6.97 (d, *J* = 7.5 Hz, 1H), 6.86 (s, 1H), 6.60 (d, *J* = 7.9 Hz, 1H), 5.74 (s, 1H), 4.81 (s, 1H), 3.86 (s, 3H), 2.93 (s, 3H), 2.42 (s, 3H); ^{13}C NMR ($CDCl_3$, 75 MHz): δ 163.6, 160.6, 159.6, 152.1, 145.2, 139.9, 135.7, 135.6, 133.7, 130.9, 129.6, 128.4, 128.2, 126.9, 123.7, 120.8, 119.2, 115.3, 114.7, 114.4, 114.2, 73.5, 55.4, 32.2, 15.6; HRMS (ESI) calcd for $C_{26}H_{22}N_2O_4$ [M + H]$^+$, 427.1652, found 427.1650.

*4.3.**5. 2- (3- (3, 4-dimethoxyphenyl) -8-methyl -2 -oxo- 2H- chromen- 6-yl) -3 -methyl- 2, 3- dihydroquinazolin- 4(1H)-one (10e)***

Light yellow solid; Yield: 87%; m.p.: 168-170 ºC; IR (KBr): 3415, 3013, 2921, 1635, 1252, 1026 cm^{-1}; ^{1}H NMR ($CDCl_3$, 300 MHz): δ 7.98 (d, *J* = 7.4 Hz, 1H), 7.71 (s, 1H), 7.39 (s, 1H), 7.36 (s, 1H), 7.31-7.28 (m, 3H), 6.94 (d, *J* = 8.1 Hz, 1H), 6.89-6.84 (m, 1H), 6.60 (d, *J* = 7.8 Hz, 1H), 5.75 (s,1H), 4.77 (s, 1H), 3.95 (s, 3H), 3.93(s, 3H), 2.94 (s, 3H), 2.44 (s, 3H); ^{13}C NMR ($CDCl_3$, 75 MHz): δ 163.7, 160.6, 151.9, 149.9, 148.8, 145.1, 138.6, 135.6, 133.7, 130.5, 128.5, 127.9, 127.0, 126.9, 123.4, 121.3, 119.5, 119.3, 115.4, 114.4, 111.6, 111.3, 75.3, 56.1, 32.2, 15.6; HRMS (ESI) calcd for $C_{27}H_{24}N_2O_5$ [M + H]$^+$, 457.1758, found 457.1755.

*4.3.**6. 3- Methyl -2 - (8-methyl-2-oxo-3- (3, 4, 5-trimethoxyphenyl) -2H-chromen-6-yl) -2, 3- dihydroquinazolin-4(1H)-one (10f)***

Yellow solid; Yield: 85%; m.p.: 178-180 ºC; IR (KBr):3402, 3018, 2929, 1641, 1216, 1047 cm^{-1}; ^{1}H NMR ($CDCl_3$, 300 MHz): δ 7.97 (d, *J* = 7.6 Hz, 1H), 7.74 (s, 1H), 7.40 (s, 1H), 7.36 (s, 1H), 7.29-7.25 (m, 1H), 6.94 (s, 2H), 6.88- 6.83 (m, 1H), 6.59 (d, *J* = 7.8 Hz, 1H), 5.75 (s, 1H), 4.85 (s, 1H), 3.92 (s, 3H), 3.89 (s, 6H), 2.95 (s, 3H), 2.45 (s, 3H); ^{13}C NMR (DMSO-d_6, 75 MHz): δ 159.0, 155.7, 148.5, 147.3, 140.5, 134.8, 134.3, 131.0, 129.1, 126.2, 125.2, 123.8, 123.4, 122.2, 118.8, 114.7, 114.5, 110.7, 109.8, 101.3, 68.7, 56.2, 51.7, 27.6, 10.8; HRMS (ESI) calcd for $C_{28}H_{26}N_2O_6$ [M + H]$^+$, 487.1864, found 487.1857.

*4.3.**7. 2- (3-(benzo[d] [1, 3] dioxol-5-yl) -8-methyl-2-oxo-2H-chromen-6-yl) -3-methyl-2, 3-dihydroquinazolin- 4(1H)-one (10g)***

White solid; Yield: 84%; m.p.: 165-167 ºC; IR (KBr): 3412, 3011, 2921, 1634, 1243, 1039 cm^{-1}; ^1H NMR ($CDCl_3$, 300 MHz): δ 7.95 (d, J = 7.6 Hz, 1H), 7.64 (s, 1H), 7.38 (s, 1H), 7.32 (s, 1H) 7.28-7.24 (m, 1H), 7.19-7.14 (m, 2H), 6.88-6.82 (m, 2H), 6.58 (d, J = 7.9 Hz, 1H), 6.00 (s, 2H), 5,73 (s, 1H), 4.77 (s, 1H), 2.91 (s, 3H), 2.40 (s, 3H); ^{13}C NMR ($CDCl_3$, 75 MHz): δ 163.6, 160.5, 151.9, 148.4, 147.8, 145.2, 138.9, 135.7, 133.7, 130.6, 128.4, 128.2, 127.9, 126.8, 123.5, 122.5, 119.4, 119.2, 115.3, 114.4, 108.9, 108.4, 101.5, 73.5, 32.3, 15.6; HRMS (ESI) calcd for $C_{26}H_{20}N_2O_5$ $[M + H]^+$, 441.1445, found 441.1447.

*4.3.**8. 2-(3-(2-chlorophenyl)-8-methyl-2-oxo-2H-chromen-6-yl)-3-methyl-2,3-dihydroquinazolin 4(1H)-one (10h)***

White solid; yield: 83%; m.p.: 228-230 ºC; IR (KBr): 3408, 3025, 2946, 1670, 1220, 1052 cm^{-1}; ^1H NMR (DMSO-d_6, 300 MHz): δ 8.13 (s, 1H), 7.66 (d, J = 7.2 Hz, 1H), 7.55-7.45 (m, 6H), 7.31 (s, 1H), 7.23-7.19 (m, 1H), 6.69-6.64 (m, 2H), 5.91 (s, 1H), 2.88 (s, 3H), 2.40 (s, 3H); ^{13}C NMR (DMSO-d_6, 75 MHz): δ 162.9, 159.2, 152.1, 146.6, 143.6, 137.1, 134.4, 133.7, 133.2, 132.2, 131.7, 130.8, 129.7, 127.9, 127.7, 126.9, 126.1, 124.4, 118.8, 117.7, 114.8, 114.6, 71.8, 32.5, 15.6; HRMS (ESI) calcd for $C_{25}H_{19}ClN_2O_3$ $[M + H]^+$, 431.1157, found 431.1149.

*4.3.**9. 3- methyl-2- (8-methyl-3-(2-nitrophenyl) -2-oxo-2H-chromen-6-yl) -2, 3-dihydroquinazolin 4(1H)-one (10i)***

Light yellow solid; Yield: 82%; m.p.: 188-190 ºC; IR (KBr): 3441, 3015, 2944, 1660, 1220, 1032 cm^{-1}; ^1H NMR (DMSO-d_6, 300 MHz): δ 8.34 (s, 1H), 8.13 (s, 1H), 7.86 (s, 1H) 7.71 (s, 3H), 7.57 (d, J = 7.4 Hz, 2H), 7.39 (s, 1H), 7.22 (s, 1H), 6.67 (s, 2H), 5.95 (s, 1H), 2.92 (s, 3H), 2.40 (s, 3H); ^{13}C NMR (DMSO-d_6, 100 MHz): δ 163.0, 159.5, 151.7, 148.6, 146.5, 141.6, 137.4,

134.6, 133.7, 132.9, 131.9, 130.8, 129.9, 127.9, 126.8, 126.2, 124.8, 124.2, 119.1, 117.7, 114.8, 114.6, 71.8, 32.5, 15.5; HRMS (ESI) calcd for $C_{25}H_{19}N_3O_5$ $[M + H]^+$, 442.1397, found 442.1379.

4.3.10. 3- methyl- 2- (8-methyl-2-oxo-3- (thiophen-2-yl)-2H-chromen-6-yl)-2, 3-dihydroquinazolin-4(1H)-one (10j)

Green solid; Yield: 84%; m.p.: 178-180 ºC; IR (KBr): 3410, 2921, 1611, 1213 cm^{-1}; ^1H NMR (DMSO-d_6, 300 MHz): δ 8.59 (s, 1H), 7.89-7.88 (m, 1H), 7.69-7.66 (m, 2H), 7.51 (s, 2H), 7.37-7.36 (m, 1H), 7.24-7.16 (m, 2H), 6.70-6.63 (m, 2H), 5.92-5.91 (m, 1H), 2.91 (s, 3H), 2.38 (s, 3H); ^{13}C NMR (DMSO-d_6, 75 MHz): δ 163.0, 159.4, 150.9, 146.6, 137.2, 136.7, 133.7, 131.2, 129.4, 128.0, 127.8, 127.3, 125.9, 123.8, 121.1, 119.3, 117.7, 114.9, 114.7, 71.9, 32.6, 15.6; HRMS (ESI) calcd for $C_{23}H_{18}N_2O_3S$ $[M + H]^+$, 403.1111, found 403.1104.

4.3.11. 2- (3- (3, 4-dimethoxyphenyl) -8-ethyl-2-oxo-2H-chromen-6-yl) -3-methyl-2, 3-dihydro quinazolin-4(1H)-one (10k)

Yellow solid; Yield: 86%; m.p.: 95-97 ºC; IR (KBr): 3409, 2921, 1611, 1213 cm^{-1} ; ^1H NMR ($CDCl_3$, 300 MHz): δ 7.99 (d, J = 7.7 Hz, 1H), 7.72 (s, 1H), 7.41 (s, 1H), 7.37 (s, 1H), 7.29-7.26 (m, 3H), 6.96-6.85 (m, 2H), 6.59 (d, J = 8.0 Hz, 1H), 5.77 (s, 1H), 4.69 (s, 1H), 3.95 (s, 3H), 3.93 (s, 3H), 2.94-2.85 (m, 5H), 1.31-1.27 (m, 3H); ^{13}C NMR (DMSO-d_6, 75 MHz): δ 163.6, 160.4, 151.4, 149.9, 148.7, 145.0, 138.6, 135.6, 133.6, 132.8, 128.9, 128.4, 127.9, 127.0, 123.3, 121.2, 119.6, 119.3, 115.5, 114.3, 111.6, 111.0, 73.5, 56.0, 55.9, 32.1, 22.5, 14.0; HRMS (ESI) calcd for $C_{28}H_{25}N_2O_5$ $[M + H]^+$, 471.1914, found 471.1911.

4.3.12. 2- (3- (3, 4-dimethoxyphenyl)-2-oxo-8-propyl-2H-chromen-6-yl)-3-methyl-2, 3 dihydro quinazolin-4(1H)-one (10l)

White solid; Yield: 88%; m.p.: 98-100 ºC; IR (KBr): 3410, 2921, 1611, 1213 cm^{-1}; ^1H NMR ($CDCl_3$, 300 MHz): δ 8.00 (d, J = 7.7 Hz, 1H), 7.74 (s, 1H), 7.40-7.39 (m, 2H), 7.29 (d, J = 7.7

Hz, 3H), 6.99-6.86 (m, 2H), 6.58 (d, *J* = 7.9 Hz, 1H), 5.77 (s, 1H), 4.57 (s, 1H), 3.95 (s, 3H), 3.94 (s, 3H), 2.95 (s, 3H), 2.88-2.83 (m, 2H), 1.78-1.68 (m, 2H), 1.01-0.97 (m, 3H); ^{13}C NMR ($CDCl_3$, 75 MHz): δ 163.6, 160.4, 151.5, 149.8, 148.7, 144.9, 138.6, 135.4, 133.6, 131.3, 129.7, 128.4, 128.0, 127.0, 123.4, 121.2, 119.7, 119.3, 115.5, 114.3, 111.6, 111.0, 73.4, 56.0, 32.1, 22.8, 13.8; HRMS (ESI) calcd for $C_{29}H_{28}N_2O_5$ $[M + H]^+$, 485.2071, found 485.2073.

*4.3**.13. 2-(3-(3, 4-dimethoxyphenyl)-8-isopropyl-2-oxo-2H-chromen-6-yl) -3-methyl-2, 3 dihydro quinazolin-4(1H)-one (10m)***

Light yellow solid; Yield: 88%; m.p.: 110-112 ºC; IR (KBr): 3419, 3017, 2931, 1639, 1217, 1026 cm^{-1}; ^{1}H NMR ($CDCl_3$, 300 MHz): δ 8.00-7.98 (m, 1H), 7.74 (s, 1H), 7.47 (d, *J* = 1.5 Hz, 1H), 7.38 (d, *J* = 1.7 Hz, 1H), 7.32-7.26 (m, 3H), 6.96-6.93 (m, 1H), 6.90-6.85 (m, 1H), 6.59 (s, *J* = 7.9 Hz, 1H), 5.78 (s, 1H), 4.65 (s, 1H), 3.95 (s, 3H), 3.93 (s, 3H), 3.69-3.60 (m, 1H), 2.94 (s, 3H), 1.33-1.32 (m, 3H), 1.31-1.30 (m, 3H); ^{13}C NMR ($CDCl_3$, 75 MHz): δ 163.6, 160.4, 150.9, 149.8, 148.7, 145.0, 138.8, 137.3, 135.6, 133.6, 128.4, 127.9, 127.0, 126.4, 123.2, 121.2, 119.7, 119.3, 115.5, 114.3, 111.5, 111.0, 73.5, 55.9, 32.1, 26.7, 22.6; HRMS (ESI) calcd for $C_{29}H_{28}N_2O_5$ $[M + H]^+$, 485.2071, found 485.2056.

*4.3.14. 2- (8-tert-butyl-3- (3, 4-dimethoxyphenyl) -2-oxo-2H-chromen-6-yl) -3-methyl-2, 3-dihydro quinazolin-4(1H)-one (**10n**)*

Light yellow solid; Yield: 86%; m.p.: 115-117 ºC; IR (KBr): 3410, 2921, 1611, 1213 cm^{-1} ;^{1}H NMR ($CDCl_3$, 300 MHz): δ 8.01-7.99 (m, 1H), 7.75 (s, 1H), 7.53 (d, *J* = 1.6 Hz, 1H), 7.40 (d, *J* = 1.6 Hz, 1H), 7.35-7.26 (m, 3H), 6.96-6.86 (m, 2H), 6.59 (d, *J* = 7.9 Hz, 1H), 5.77 (s, 1H), 4.61 (s, 1H), 3.95 (s, 3H), 3.94 (s, 3H), 2.95 (s, 3H), 1.52 (s, 9H); ^{13}C NMR ($CDCl_3$, 75 MHz): δ 162.9, 159.6, 151.6, 149.8, 148.8, 146.7, 140.3, 137.3, 136.7, 133.7, 127.4, 127.1, 126.2, 124.5,

121.7, 120.3, 117.6, 114.9, 114.6, 112.5, 111.8, 72.0, 56.1, 56.0, 39.3, 35.0, 32.5, 29.9; HRMS (ESI) calcd for $C_{30}H_{30}N_2O_5$ $[M + H]^+$, 499.2227, found 499.2218.

*4.3.**15. 2- (8-sec-butyl-3-(3, 4-dimethoxyphenyl) -2-oxo-2H-chromen-6-yl) -3-methyl-2, 3-dihydro quinazolin-4(1H)-one (10o)***

White solid; Yield: 89%; m.p.: 113-115 ºC; IR (KBr): 3421, 3019, 2925, 1641, 1216, 1027 cm^{-1}; ^1H NMR ($CDCl_3$, 300 MHz) : δ 8.01-7.99 (m, 1H), 7.75 (s, 1H), 7.45-7.43 (m, 1H), 7.40-7.39 (m, 1H), 7.32-7.28 (m, 3H), 6.97-6.87 (m, 2H), 6.59 (d, J = 7.9 Hz, 1H), 5.79 (s, 1H), 4.55 (s, 1H) 3.96 (s, 3H), 3.94 (s, 3H), 3.48-3.41 (m, 1H), 2.94 (s, 3H),1.31-1.28 (m, 5H), 0.89 (t, J = 7.0 Hz, 3H); ^{13}C NMR ($CDCl_3$, 75 MHz): δ 163.7, 160.5, 151.3, 149.9, 148.8, 145.1, 138.9, 136.3, 135.6, 133.7, 128.5, 128.1, 127.1, 123.4, 121.3, 119.9, 119.5, 115.8, 114.4, 111.7, 111.1, 73.6, 56.0, 33.5, 32.2, 29.7, 20.5, 12.0; HRMS (ESI) calcd for $C_{30}H_{30}N_2O_5$ $[M + H]^+$, 499.2227, found 499.2189.

*4.3.**16. 2- (3- (3, 4-dimethoxyphenyl)-2-oxo-7, 8, 9, 10-tetrahydro-2H-benzo[h]chromen-6-yl) -3-methyl-2, 3-dihydroquinazolin-4(1H)-one (10p)***

Yellow solid; Yield: 86%; m.p.: 125-127 ºC; IR (KBr): 3425, 3015, 2934, 1650, 1190, 1042 cm^{-1}; ^1H NMR ($CDCl_3$, 300 MHz): δ 8.00 (d, J = 7.5 Hz, 1H), 7.72 (s, 1H), 7.36-7.25 (m, 5H), 6.95-6.85 (m, 2H), 6.57 (d, J = 7.9 Hz, 1H), 6.07 (s, 1H), 4.51 (s, 1H), 3.96 (s, 3H), 3.93 (s, 3H), 3.03-2.92 (m, 6H), 1.90 (bs, 5H); ^{13}C NMR ($CDCl_3$, 75 MHz): δ 164.1, 160.6, 151.3, 149.6, 148.7, 145.1, 139.1, 138.7, 133.5, 132.5, 128.4, 127.1, 126.8, 126.4, 123.3, 121.1, 119.2, 116.9, 115.5, 114.6, 111.4, 110.9, 70.4, 55.9, 31.8, 26.6, 23.1, 22.3, 21.3; HRMS (ESI) calcd for $C_{30}H_{28}N_2O_5$ $[M + H]^+$, 497.2071, found 497.2056.

4.4. ***General procedure for the synthesis of compound 11*****:**

Compound **11** was synthesized according to the literature procedure [25]. Briefly, a mixture of 4-hydroxy-5-methylisophthalaldehyde (**8a,** 1.0 mmol), methylamine (1.5 mmol) and isatoicanhydride (1.0 mmol) in acetic acid (5.0 mL) was stirred in a round-bottom flask for 2.0 h at 110 °C (initially effervescence was observed due to the generation of CO_2 gas). Upon completion of the reaction, the reaction mixture was diluted with water (25 mL), followed by extraction with $CHCl_3$ (2x25 mL). The combined organic phases were dried over anhydrous Na_2SO_4 and concentrated *in vacuo*. The crude product was purified by column chromatography on silica gel (100-200) in 40% DCM/Hexane solvent system. The required compound **11** was thus obtained.

4.5. ***General synthesis of coumarin derivatives (12a and 12b):***

A solution of 2-hydroxy-3-methyl-5-(3-methyl-4-*oxo*-1, 2, 3, 4-tetrahydroquinazolin-2-yl) benzaldehyde (**9a**, 1.0 mmol), dimetylmalanoate/dimethylmalanoate (1.1 mmol) in absolute ethanol (10 mL) was treated with piperidine (0.20 mL) and refluxed for 30 min. Most of the excess reagent was evaporated under reduced pressure, and the residue was suspended in water (20 mL) and extracted 3-fold with $CHCl_3$ (15 mL). The combined organic layers were dried on Na_2SO_4, filtered, and concentrated to dryness under reduced pressure. The crude product thus obtained was purified by column chromatography (60-120 mesh) using hexane/ethylacetate (90:10, v/v) as eluent to furnish compound **12a** and **12b**.

*4.5.****1. Methyl 8-methyl-6-(3-methyl-4-oxo-1, 2, 3, 4-tetrahydroquinazolin-2-yl)-2-oxo-2H-chromene-3-carboxylate (12a)***

White solid; yield: 90%; m.p.: 213-215 ºC; IR (KBr): 3015, 2934, 1650, 1190, 1042 cm^{-1}; ^1H NMR ($CDCl_3$, 300 MHz): δ 8.45 (s, 1H), 7.97 (d, J = 7.6 Hz, 1H), 7.55 (s, 1H), 7.42 (s, 1H),

7.31-7.28 (m, 1H), 6.91-6.86 (m, 1H), 6.61 (d, *J* = 8.0 Hz, 1H), 5.76 (s, 1H), 4.75 (s, 1H), 3.95 (s, 3H), 2.93 (s, 3H), 2.43 (s, 3H); ^{13}C NMR ($CDCl_3$, 75 MHz): δ 163.5, 163.3, 156.5, 153.7, 148.9, 145.0, 136.3, 133.7, 128.3, 127.4, 125.1, 119.2, 117.8, 117.4, 115.1, 114.5, 73.0, 52.9, 32.2, 15.4; HRMS (ESI) calcd for $C_{21}H_{18}N_2O_5$ [M + H]$^+$, 379.1288, found 379.1286.

4.5.2. Ethyl 8-methyl-6-(3-methyl-4-oxo-1, 2, 3, 4-tetrahydroquinazolin-2-yl)-2-oxo-2H-chromene-3-carboxylate (12b)

White solid; yield: 90%; m.p.: 218-220 ºC; IR (KBr): 3025, 2944, 1660, 1220, 1042 cm^{-1}; ^{1}H NMR ($CDCl_3$, 300 MHz): δ 8.38 (s, 1H), 7.94 (d, *J* = 7.7 Hz, 1H), 7.52 (s, 1H), 7.40 (s, 1H), 7.30-7.25 (m, 1H), 6.88-6.83 (m, 1H), 6.64 (d, *J* = 8.0 Hz, 1H), 5.75 (s, 1H), 5.03 (s, 1H), 4.40 (q, *J* = 7.0 Hz, 2H), 2.91 (s, 3H), 2.38 (s, 3H), 1.41 (t, *J* = 7.1 Hz, 3H); ^{13}C NMR ($CDCl_3$, 75 MHz): δ 163.5, 162.6, 156.6, 153.6, 148.4, 145.2, 136.4, 133.8, 128.3, 127.4, 125.1, 119.1, 118.1, 117.4, 115.1, 114.6, 73.1, 62.1, 32.2, 15.5, 14.2; HRMS (ESI) calcd for $C_{22}H_{20}N_2O_5$ [M + H]$^+$, 393.1445, found 393.1440.

4.6. General synthetic procedure for preparation of benzofuran (13a and 13b):

To a mixture of 2-hydroxy-3-methyl-5-(3-methyl-4-oxo-1, 2, 3, 4-tetrahydroquinazolin-2-yl) benzaldehyde (**11**, 1.0 mmol) and phenacyl bromide (1.0 mmol) in acetonitrile (5 mL) K_2CO_3 (5.0 mmol) was added and resulting reaction mixture was refluxed for 4.0 h (monitor by TLC). After completion of reaction the excess solvent was removed, diluted with water (10 mL) and extracted 3-fold with $CHCl_3$ (15 mL). The combined organic layers were dried on Na_2SO_4, filtered, and concentrated to dryness under reduced pressure. The residue was purified over column chromatography (silica, 100-200 mesh, hexane/DCM) provided the pure compounds.

***4.6.1. 3-methyl-2-(7-methyl-2-(4-methylbenzoyl)benzofuran-5-yl)-2, 3-dihydroquinazolin-4(1H)-one* (13a)**

White solid; yield: 70%; m.p.: 235-237 ºC; IR (KBr): 3025, 2946, 1670, 1240, 1062 cm^{-1}; ^1H NMR ($CDCl_3$, 300 MHz): δ 7.97-7.94(m, 2H), 7.53 (s, 1H), 7.44 (s, 1H), 7.36-7.32 (m, 2H), 7.26 (s, 1H), 6.87-6.82 (m, 1H), 6.56(d, J = 7.5 Hz, 1H), 5.80 (s, 1H), 4.64 (s, 1H), 2.88 (s, 3H), 2.57 (s, 3H), 2.46 (s, 3H); ^{13}C NMR ($CDCl_3$, 75 MHz): δ 183.8, 163.7, 155.4, 153.1, 145.3, 144.1, 135.6, 134.4, 133.5, 129.7, 129.3, 128.5, 128.2, 127.4, 126.7, 123.9, 119.1, 119.0, 116.2, 114.1, 74.2, 31.9, 21.7, 15.3; HRMS (ESI) calcd for $C_{26}H_{22}N_2O_3$ $[M + H]^+$, 411.1703, found 411.1715.

4.6.2. 2-(2-(4-chlorobenzoyl)-7-methylbenzofuran-5-yl)-3-methyl-2, 3-dihydroquinazolin-4(1H)-one **(13b)**

White solid; yield: 72%; m.p.: 245-247 ºC; IR (KBr): 3025, 2946, 1670, 1220, 1052 cm^{-1}; ^1H NMR ($CDCl_3$, 300 MHz): δ 8.05-7.98 (m, 3H), 7.57-7.52 (m, 5H), 7.41 (s, 1H), 7.28 (s, 1H), 6.90-6.85 (s, 1H), 6.57 (d, J = 7.9 Hz, 1H), 5.83 (s, 1H), 4.58 (s, 1H), 2.91 (s, 3H), 2.60 (s, 3H); ^{13}C NMR ($CDCl_3$, 75 MHz): δ 182.7, 163.7, 155.5, 152.8, 145.3, 139.7, 135.9, 135.3, 133.6, 131.0, 129.0, 128.5, 127.7, 126.6, 123.9, 119.2, 119.1, 116.6, 115.4, 114.2, 74.2, 32.0, 15.3; HRMS (ESI) calcd for $C_{25}H_{19}ClN_2O_3$ $[M + H]^+$, 431.1157, found 431.1155.

4.7. General procedure for the synthesis of compounds enamine (14a and 14b):

A mixture of 2-hydroxy-3-methyl-5-(3-methyl-4-*oxo*-1, 2, 3, 4-tetrahydroquinazolin-2-yl)benzaldehyde (**9a**, 1.0 mmol) and aromatic aniline (1.0 mmol) in ethanol were stirred for 10 minute at room temperature. The resulted solid was filtered, washed with excess ethanol and dried under vacuum to obtain the respective compounds **14a** and **14b** in excellent yields.

4.7*.1. (E)-3-methyl-2-(5-methyl-4-oxo-3-((p-tolylamino)methylene)cyclohexa-1,5-dienyl)-2, 3-dihydroquinazolin-4(1H)-one* ***(14a)***

Red solid; yield: 85%; m.p.: 265-267 ºC; IR (KBr): 3421, 3025, 2946, 1670, 1220, 1052 cm^{-1}; ^1H NMR ($CDCl_3$ + DMSO-d_6, 300 MHz): δ 13.92 (s, 1H), 8.59 (s, 1H), 7.98 (d, J = 7.5 Hz, 1H),

7.31-7.21 (m, 7H), 6.89-6.84 (m, 1H), 6.58 (d, *J* = 7.9 Hz, 1H), 5.69 (s, 1H), 4.51 (s, 1H), 2.89 (s, 3H), 2.40 (s, 3H), 2.32 (s, 3H); ^{13}C NMR ($CDCl_3$+DMSO-d_6 75 MHz): δ 162.2, 160.4, 158.5, 145.2, 143.8, 135.6, 132.0, 131.0, 129.0, 128.7, 126.9, 126.5, 125.1, 119.8, 116.6, 116.2, 113.3, 113.0, 71.6, 30.5, 19.7, 14.4; HRMS (ESI) calcd for $C_{24}H_{23}N_3O_2$ $[M + H]^+$, 386.1863, found 386.1850.

4.7.2. (E)-2-(3-((4-chlorophenylamino)methylene)-5-methyl-4-oxocyclohexa-1,5-dienyl)-3-methyl-2, 3-dihydroquinazolin-4(1H)-one (14b)

Red solid; yield: 86%; m.p.: 275-277 ºC; IR (KBr): 3420, 3015, 2943, 1650, 1230, 1052 cm^{-1}; ^{1}H NMR ($CDCl_3$, 300 MHz): δ 13.51(s, 1H), 8.57 (s, 1H), 7.99 (d, *J* = 6.7 Hz, 1H), 7.42-7.21 (m, 7H), 6.90-6.85 (m, 1H), 6.58 (d, *J* = 7.6 Hz, 1H), 5.70 (s, 1H), 4.49 (s, 1H), 2.91 (s, 3H), 2.32 (s, 3H); ^{13}C NMR ($CDCl_3$, 100 MHz): δ 163.7, 162.4, 160.3, 146.5, 145.1, 133.5, 133.5, 132.8, 132.6, 129.6, 128.6, 128.2, 127.5, 122.4, 119.3, 118.0, 115.6, 114.1, 73.7, 31.8, 15.6; HRMS (ESI) calcd for $C_{23}H_{20}ClN_3O_2$ $[M + H]^+$, 406.1317, found 406.1311.

5. Pharmacology

5.1. Animals model

All *in vivo* experiments and procedures were performed in accordance with the guidelines established in the guide for the care and use of laboratory animals and were approved by the Institutional Animal Ethics Committee (IAEC) of CSIR-Central Drug Research Institute, Lucknow, India. The IAEC is certified by Animal Welfare Board of India (AWBI) and Committee for the Purpose of Supervision and Control of Experiments on Animals (CPCSEA), which are statutory bodies of Government of India. For development of high fat diet (HFD) induced obesity, taken five to six weeks old C57BL/6J male mice with 22-25g body weight were fed with 60% fat diet (Research diet Inc; D12492) for 10 weeks, and an experimental

controls group were fed with normal chow (10% fat diet, Research diets Inc; Cat no. D12450). Animals were housed in a 12- h light/dark cycle (lights on at 8.00 am) at 22^0C.

5.2. Drugs treatment

Lorcaserin HCl (Catalog No.S4109) was purchased from Selleck Chemical's. For mice treatment initially Lorcaserin and compound **10c** dissolved in 100% DMSO then mixed in 5% Gum acacia (Fisher Scientific) solution of normal saline (working DMSO concentration < 5%). Lorcaserin (10 mg/kg body weight) and compound **10c** (20 mg/kg body weight) was administrated through oral route for six weeks.

5.3. Intra-peritoneal glucose tolerance test (IPGTT)

Diet-induced obese and non-obese C57BL/6J mice fasted for sixteen hours and fasting blood glucose baseline was measured with a glucose meter (Accu-Chek Active Kit of Roche Products India Pvt. Ltd.) by tail-tip amputation. Then mice were treated with glucose (2g/kg body weight) by intraperitoneal injection. After the glucose administration, blood glucose level was measured at different time points 15' 30' 60' 90' and 120 minutes.

5.4. Serum Lipid profiling

Animals were euthanized following six weeks treatment. Blood plasma samples were collected by cardiac puncture into 3.8% sodium citrate buffer under the overdose of anesthesia (350 mg/kg of avertin), followed by decapitation. Blood was centrifuged immediately after collection for 15 min at 4000 rpm and blood serum stored at -80°C for biochemical analysis. Blood serum TG, TC, HDLc, and LDLc were estimated using Merck selectra junior bio-analyzer (Merck Millipore).

5.5. Leptin ELISA

Plasma Leptin levels were measured using the mouse DuoSet kits (R&D Systems) following the manufacturer's instructions.

5.6. Measurements of fat mass and lean mass

Body weight of mouse was measured at every 3rd day during the experiment, and body fat composition was determined at the end of the experiment using specialized nuclear magnetic resonance (NMR)-Magnetic resonance imaging-based technology -Echo MRI (Echo Medical Systems).

5.7. GloSensor assay

All synthesized compound's activity were evaluated at GPR109a receptor by GloSensor assay according to the previously described method with some modifications [38]. In this assay HEK293T cells transiently transfected with 5.0µg human GPR109a receptor plasmid DNA and 5.0µg glosensor-22F cAMP plasmid DNA (Cat. No. E2301, Promega Corp.). Transfected cells were plated in 96 well tissue culture plate with complete high glucose DMEM media (containing 5% FBS) and incubated at 37^{0}C tissue culture incubator with 5% CO_2 for overnight. After the overnight incubation, media was discarded from culture plate and added luciferin solution, and then cells were incubated for 60 min in tissue culture incubator at 37^{0}C. After 60 min incubation, cells were treated with compounds and NA at different concentrations. Finally, cells were stimulated with 10µM forskolin for 10 min, and luminescence was measured using multimode plate reader (BMG, Labtech) and normalize luminescence data were analyzed using GraphPad Prism 5.0 to calculate EC_{50} values.

5.8. β -arrestin Tango assay

It is a cell-based assay to quantify ligand-dependent β-arrestin2 recruitment assay [39]. β-arrestin recruitment was measured by previously described "Tango" assay method [38]. Briefly, HTLA cells (kind gift from Dr. Gilad Barnea, Brown University, USA) were transiently transfected with human GPR109a-Tango receptor plasmid DNA (Kind gift from Dr. Bryan Roth, UNC-Chapel Hill, USA) and plated in 96 well tissue culture plate with high glucose media containing 5% fetal bovine serum. Transfected cells were incubated at 37℃ with 5% CO_2 in a humidified incubator for six hours. After six hours incubation, cells were treated with drugs at different doses and further incubated for overnight. Finally, discard the media from treated cell culture plate and add 100mL of BrightGlo substrate (Cat. No. E2620, Promega) to each well of 96 well plates. After the BrightGlo addition luminescence was measured using multimode plate reader (BMG, Labtech) and normalize luminescence data were analyzed using GraphPad Prism 5.0 to calculate EC_{50} values.

5.9. Molecular modeling and docking studies

Homology models of *Homo sapiens* Nicotinic acid receptor GPR109a were constructed for molecular interaction studies. The sequence of GPR109a was extracted from UniProt (ID-Q8TDS4), and the blast was performed to find suitable templates for building a homology model of this receptor protein. The X-ray crystal structure of *Mus musculus* active μ-opioid receptor bound to an agonist BU72 was selected as a template (PDB identifier: 5C1M) [40]. GPR109a shares 30% sequence identity with the template protein. Ten models of GPR109a were generated using Modeller 9.14 package [41]. 26 residues at N-terminal and 56 residues at C-terminal of GPR109a were eliminated due to lack of proper alignment with the template. Moreover, these

terminal residues are not involved in binding a ligand. For molecular visualization UCSF Chimera 1.10.2 was used [42]. The chemical structures of (R) and (S) isomers of the compound were sketched using SYBYL-X 2.1.1 and further energy minimization was done with 1000 iterations using MMFF94 force field [43]. For further optimization, GPR109a protein was embedded in the pre-equilibrated lipid bilayer (POPC) [44] followed by energy minimization using Gromacs v5.0.7 with 1000 cycles of steepest descent algorithm. All the docking studies were done with Autodock 4.2 using Lamarckian genetic algorithm [45]. A grid of 92, 98 and 82 points was made in the x, y and z directions respectively. Numbers of docking runs were set to 200 for each isomer. All the other docking parameters were set as default. Non-bonded interaction studies for docked structures were carried out using non-bonded module of Discovery Studio 4.1 [46].

5.10. Data Analysis

Statistical analysis was performed using GraphPad Prism 5 software (La Jolla, California, USA).

Acknowledgements

We wish to thank the Director, CSIR-CDRI for his constant support and encouragement in drug development program, Dr. S.P. Singh for technical support, SAIF for NMR, IR, and Mass spectral data. L.R.S. and G.R.P. are thankful to CSIR, New Delhi, and A.K is thankful to UGC, New Delhi, India for financial support. We acknowledge the financial support of CSIR network project BSC0102 (THUNDER).

Author Contributions

[#]Singh L R and Kumar A contributed equally. The manuscript was written through contributions of all authors. All authors have approved the final version of the manuscript.

References:

1. P.L. Canner, K.G. Berge, N.K. Wenger, J. Stamler, L. Friedman, R.J. Prineas, W. Friedewald, Fifteen year mortality in Coronary Drug Project patients: long-term benefit with niacin, J. Am. Coll. Cardiol. 8 (1986) 1245-1255.
2. E. Bruckert, J. Labreuche, P. Amarenco, Meta-analysis of the effect of nicotinic acid alone or in combination on cardiovascular events and atherosclerosis, Atherosclerosis, 210 (2010) 353-361.
3. N.B. Pike, Flushing out the role of GPR109a (HM74A) in the clinical efficacy of nicotinic acid, J. Clin. Invest. 115 (2005) 3400-3403.
4. T. Soga, M. Kamohara, J. Takasaki, S. Matsumoto, T. Saito, T. Ohishi, H. Hiyama, A. Matsuo, H. Matsushime, K. Furuichi, Molecular identification of nicotinic acid receptor, Biochem. Biophys. Res. Commun. 303 (2003) 364-369.
5. S. Tunaru, J. Kero, A. Schaub, C. Wufka, A. Blaukat, K. Pfeffer, S. Offermanns, PUMA-G and HM74 are receptors for nicotinic acid and mediate its anti-lipolytic effect, Nat. Med. 9 (2003) 352-355.
6. A. Wise, S.M. Foord, N.J. Fraser, A.A. Barnes, N. Elshourbagy, M. Eilert, D.M. Ignar, P.R. Murdock, K. Steplewski, A. Green, A.J. Brown, S.J. Dowell, P.G. Szekeres, D.G. Hassall, F.H. Marshall, S. Wilson, N.B. Pike, Molecular identification of high and low affinity receptors for nicotinic acid, J. Biol. Chem. 278 (2003) 9869-9874.
7. M. Rahman, S. Muhammad, M.A. Khan, H. Chen, D.A. Ridder, H. Muller-Fielitz, B. Pokorna, T. Vollbrandt, I. Stolting, R. Nadrowitz, J.G. Okun, S. Offermanns, M. Schwaninger, The beta-hydroxybutyrate receptor HCA2 activates a neuroprotective subset of macrophages, Nature comm. 5 (2014) 3944.
8. Z. Benyo, A. Gille, C.L. Bennett, B.E. Clausen, S. Offermanns, Nicotinic acid-induced flushing is mediated by activation of epidermal langerhans cells, Mol. Pharma. 70 (2006) 1844-1849.
9. J.D. Morrow, J.A. Awad, J.A. Oates, L.J. Roberts, 2nd, Identification of skin as a major site of prostaglandin D2 release following oral administration of niacin in humans, J. Invest. Dermat. 98 (1992) 812-815.
10. R.W. Walters, A.K. Shukla, J.J. Kovacs, J.D. Violin, S.M. DeWire, C.M. Lam, J.R. Chen, M.J. Muehlbauer, E.J. Whalen, R.J. Lefkowitz, beta-Arrestin1 mediates nicotinic

acid-induced flushing, but not its antilipolytic effect, in mice, J. Clin. Invest. 119 (2009) 1312-1321.

11. B. Lauring, A.K.P. Taggart, J.R. Tata, R. Dunbar, L. Caro, K. Cheng, J. Chin, S.L. Colletti, J. Cote, S. Khalilieh, J.J. Liu, W.L. Luo, A.A. MacLean, L.B. Peterson, A.B. Polis, W. Sirah, T.J. Wu, X. Liu, L. Jin, K. Wu, P.D. Boatman, G. Semple, D.P. Behan, D.T. Connolly, E. Lai, J.A. Wagner, S.D. Wright, C. Cuffie, Y.B. Mitchel, D.J. Rader, J.F. Paolini, M.G. Waters, A. Plump, Niacin Lipid Efficacy Is Independent of Both the Niacin Receptor GPR109A and Free Fatty Acid Suppression, Sci. Transl. Med., 4 (2012).
12. D. Wanders, E.C. Graff, B.D. White, R.L. Judd, Niacin increases adiponectin and decreases adipose tissue inflammation in high fat diet-fed mice, PloS one, 8 (2013) e71285.
13. Y. Arita, S. Kihara, N. Ouchi, M. Takahashi, K. Maeda, J. Miyagawa, K. Hotta, I. Shimomura, T. Nakamura, K. Miyaoka, H. Kuriyama, M. Nishida, S. Yamashita, K. Okubo, K. Matsubara, M. Muraguchi, Y. Ohmoto, T. Funahashi, Y. Matsuzawa, Paradoxical decrease of an adipose-specific protein, adiponectin, in obesity, Biochem. and Biophys. Research comm. 257 (1999) 79-83.
14. E.H. Jeninga, A. Bugge, R. Nielsen, S. Kersten, N. Hamers, C. Dani, M. Wabitsch, R. Berger, H.G. Stunnenberg, S. Mandrup, E. Kalkhoven, Peroxisome proliferator-activated receptor gamma regulates expression of the anti-lipolytic G-protein-coupled receptor 81 (GPR81/Gpr81), J. Bio. Chem. 284 (2009) 26385-26393.
15. S. Offermanns, Hydroxy-Carboxylic Acid Receptor Actions in Metabolism, Trends Endocrin. Met., 28 (2017) 227-236.
16. (a) A. Conte, H. Dehmlow, U. Grether, N.A. Kratochwil, H. Kuehne, R. Narquizian, C.G. Panousis, J.U. Peters, F. Ricklin, Preparation of pyrido[2,3-d]pyrimidin-4-one derivatives as HM74A agonists, PCT Int. Appl. (2007), WO2007134986 A1 20071129; (b) A. Conte, H. Dehmlow, U. Grether, N.A. Kratochwil, H. Kuehne, R. Narquizian, C.G. Panousis, J.U. Peters, F. Ricklin, S. Roever, Novel Aza-pyridopyrimidinone derivatives, Patent Application 2007, US2008234277.
17. J. Qin, A. Rao, X. Chen, X. Zhu, Z. Liu, X. Huang, S. Degrado, Y. Huang, D. Xiao, R. Aslanian, B. Cheewatrakoolpong, H. Zhang, S. Greenfeder, C. Farley, J. Cook, S. Kurowski, Q. Li, M. van Heek, M. Chintala, G. Wang, Y. Hsieh, F. Li, A. Palani,

Discovery of a potent nicotinic Acid receptor agonist for the treatment of dyslipidemia, ACS Med. Chem. Lett. 2 (2011) 171-176.

18. (a) A. Palani, A.U. Rao, X. Chen, X. Huang, J. Su, H. Tang, Y. Huang, J. Qin, D. Xiao, S. Degrado, M. Sofolarides, X. Zhu, Z. Liu, B. McKittrick, W. Zhou, R. Aslanian, W.J. Greenlee, M. Senior, B. Cheewatrakoolpong, H. Zhang, C. Farley, J. Cook, S. Kurowski, Q. Li, M. van Heek, G. Wang, Y. Hsieh, F. Li, S. Greenfeder, M. Chintala, Discovery of SCH 900271, a Potent Nicotinic Acid Receptor Agonist for the Treatment of Dyslipidemia, ACS Med. Chem. Lett. 3 (2012) 63-68; (b) (A. Palani, J. Su, D. Xiao, X. Huang, A.U. Rao, X. Chen, H. Tang, J. Qin, Y.R. Huang, R.G. Aslanian, B.A. Mckittrick, S.J. Degrado, Ortho-condensed 2-pyridinone derivatives as nicotinic acid receptor agonists for the treatment of dyslipidemia, US2008019978, 2008.
19. S. Tejada, M. Martorell, X. Capo, J.A. Tur, A. Pons, A. Sureda, Coumarin and Derivates as Lipid Lowering Agents, Curr. Top. Med. Chem. 17 (2017) 391-398.
20. K.V. Sashidhara, G.R. Palnati, R. Sonkar, S.R. Avula, C. Awasthi, G. Bhatia, Coumarin chalcone fibrates: a new structural class of lipid lowering agents, Eur. J. Med. Chem. 64 (2013) 422-431.
21. M. Balasegaram, H. Young, F. Chappuis, G. Priotto, M. E. Raguenaud, F. Checchi, Effectiveness of Melarsoprol and Eflornithine as First-Line Regimens for Gambiense Sleeping Sickness in Nine Medecins Sans Frontieres Programmes, Trans. R. Soc. Trop. Med. Hyg. 103 (2009) 280-290.
22. (a) U. Muh, M. Schuster, R. Heim, A. Singh, E. R. Olson, E. P. Greenberg, Novel Pseudomonas Aeruginosa Quorum-Sensing Inhibitors Identified in an Ultra-High-Throughput Screen, Antimicrob. Agents Chemother. 50 (2006) 3674-3679. (b) C. Vitale, G. Mercuro, C. Castiglioni, A. Cornoldi, A. Tulli, M. Fini, M. Volterrani, G. M. Rosano, Metabolic Effect of Telmisartan and Losartan in Hypertensive Patients with Metabolic Syndrome, Cardiovasc. Diabetol. 4 (2005) 6.
23. P. Sivaprakasam, P. N. Tosso, R. J. Doerksen, Structure-Activity Relationship and Comparative Docking Studies for Cycloguanil Analogs as Pfdhfr-Ts Inhibitors, J. Chem. Inf. Model, 49 (2009), 1787-1796.

24. Z. Wang, M. Wang, X. Yao, Y. Li, J. Tan, L. Wang, W. Qiao, Y. Geng, Y. Liu, and Q. Wang, Design, Synthesis and Antiviral Activity of Novel Quinazolinones, Eur. J. Med. Chem. 53 (2012) 275-282.
25. (a) S. E. Abbas, F. M. Awadallah, N. A. Ibrahin, E. G. Said, G. M. Kamel, New Quinazolinone-Pyrimidine Hybrids: Synthesis, Anti-Inflammatory, and Ulcerogenicity Studies, Eur. J. Med. Chem. 53 (2012) 141-149. (b) K. M. Amin, M. M. Kamel, M. M. Anwar, M. Khedr, Y. M. Syam, Synthesis, Biological Evaluation and Molecular Docking of Novel Series of Spiro [(2h,3h) Quinazoline-2,1'- Cyclohexan]-4(1h)- One Derivatives as Anti-Inflammatory and Analgesic Agents, Eur. J. Med. Chem. 45 (2010) 2117-2131.
26. M. S. Mohamed, M. M. Kamel, E. M. Kassem, N. Abotaleb, S. I. Abd El-Moez, M. F. Ahmed, Novel 6,8-Dibromo-4(3h)Quinazolinone Derivatives of Anti-Bacterial and Anti-Fungal Activities, Eur. J. Med. Chem. 45 (2010) 3311-3319.
27. S. Gemma, C. Camodeca, M. Brindisi, S. Brogi, G. Kukreja, S. Kunjir, E. Gabellieri, L. Lucantoni, A. Habluetzel, D. Taramelli, N. Basilico, R. Gualdani, F. Tadini-Buoninsegni, G. Bartolommei, M. R. Moncelli, R. E. Martin, R. L. Summers, S. Lamponi, L. Savini, I. Fiorini, M. Valoti, E. Novellino, G. Campiani, S. Butini, Mimicking the Intramolecular Hydrogen Bond: Synthesis, Biological Evaluation, and Molecular Modeling of Benzoxazines and Quinazolines as Potential Antimalarial Agents, J. Med. Chem. 55 (2012) 10387-10404.
28. J. Rudolph, W. P. Esler, S. O'Connor, P. D. Coish, P. L. Wickens, M. Brands, D. E. Bierer, B. T. Bloomquist, G. Bondar, L. Chen, C. Y. Chuang, T. H. Claus, Z. Fathi, W. Fu, U. R. Khire, J. A. Kristie, X. G. Liu, D. B. Lowe, A. C. McClure, M. Michels, A. A. Ortiz, P. D. Ramsden, R. W. Schoenleber, T. E. Shelekhin, A. Vakalopoulos, W. Tang, L. Wang, L. Yi, S. J. Gardell, J. N. Livingston, L. J. Sweet, W. H. Bullock, Quinazolinone Derivatives as Orally Available Ghrelin Receptor Antagonists for the Treatment of Diabetes and Obesity, J. Med. Chem. 50 (2007) 5202-5216.
29. G. M. Chinigo, M. Paige, S. Grindrod, E. Hamel, S. Dakshanamurthy, M. Chruszcz, W. Minor, M. L. Brown, Asymmetric Synthesis of 2,3-Dihydro-2-Arylquinazolin-4-Ones: Methodology and Application to a Potent Fluorescent Tubulin Inhibitor with Anticancer Activity, J. Med. Chem. 51 (2008) 4620-4631.

30. (a) F. A. Al-Omary, L. A. Abou-Zeid, M. N. Nagi, S. E. Habib el, A. A. Abdel-Aziz, A. S. El-Azab, S. G. Abdel-Hamide, M. A. Al-Omar, A. M. Al-Obaid, H. I. El-Subbagh, Non-Classical Antifolates. Part 2: Synthesis, Biological Evaluation, and Molecular Modeling Study of Some New 2,6-Substituted-Quinazolin-4-Ones, Bioorg. Med. Chem. 18 (2010) 2849-2863. (b) G. P. Suresha, R. Suhas, W. Kapfo, D. C. Gowda, Urea/Thiourea Derivatives of Quinazolinone-Lysine Conjugates: Synthesis and Structure-Activity Relationships of a New Series of Antimicrobials, Eur. J. Med. Chem. 46 (2011) 2530-2540.
31. M. A. Ismail, S. Barker, D. A. Abou el-Ella, K. A. Abouzid, R. A. Toubar, M. H. Todd, Design and Synthesis of New Tetrazolyl- and Carboxy-Biphenylylmethyl-Quinazolin-4-One Derivatives as Angiotensin Ii At1 Receptor Antagonists, J. Med. Chem. 49 (2006) 1526-1535.
32. K.V. Sashidhara, L.R. Singh, M. Shameem, S. Shakya, A. Kumar, T.S. Laxman, S. Krishna, M.I. Siddiqi, R.S. Bhatta, D. Banerjee, Design, synthesis and anticancer activity of dihydropyrimidinone-semicarbazone hybrids as potential human DNA ligase 1 inhibitors, Medchemcomm, 7 (2016) 2349-2363.
33. K.V. Sashidhara, G.R. Palnati, S.R. Avula, A. Kumar, Efficient and General Synthesis of 3-Aryl Coumarins Using Cyanuric Chloride, Synlett, (2012) 611-621.
34. K.V. Sashidhara, G.R. Palnati, R.P. Dodda, S.R. Avula, P. Swami, One-Pot Regioselective Synthesis of Imidazole and 2,3-Dihydroquinazolinone Derivatives - An Easy Access to 'Nature-Like Molecules'; Part XIII in the Series: 'Studies on Novel Synthetic Methodologies', Synlett, 24 (2013) 1795-1800.
35. K.V. Sashidhara, L.R. Singh, D. Choudhary, A. Arun, S. Gupta, S. Adhikary, G.R. Palnati, R. Konwar, R. Trivedi, Design, synthesis and in vitro evaluation of coumarin-imidazo[1,2-a]pyridine derivatives against cancer induced osteoporosis, Rsc. Adv., 6 (2016) 80037-80048.
36. K.V. Sashidhara, R.K. Modukuri, P. Jadiya, R.P. Dodda, M. Kumar, B. Sridhar, V. Kumar, R. Haque, M.I. Siddiqi, A. Nazir, Benzofuran-chalcone hybrids as potential multifunctional agents against Alzheimer's disease: synthesis and in vivo studies with transgenic Caenorhabditis elegans, ChemMedChem, 9 (2014) 2671-2684.

37. K.V. Sashidhara, M. Kumar, R.K. Modukuri, R.K. Srivastava, A. Soni, K. Srivastava, S.V. Singh, J.K. Saxena, H.M. Gauniyal, S.K. Puri, Antiplasmodial activity of novel keto-enamine chalcone-chloroquine based hybrid pharmacophores, Bioorg. Med. Chem. 20 (2012) 2971-2981.
38. S. Dogra, C. Sona, A. Kumar, P.N. Yadav, Tango assay for ligand-induced GPCR-beta-arrestin2 interaction: application in drug discovery, Method Cell Biol. 132 (2016) 233-254.
39. G. Barnea, W. Strapps, G. Herrada, Y. Berman, J. Ong, B. Kloss, R. Axel, K.J. Lee, The genetic design of signaling cascades to record receptor activation, Proceedings of the National Academy of Sciences of the United States of America, 105 (2008) 64-69.
40. W.J. Huang, A. Manglik, A.J. Venkatakrishnan, T. Laeremans, E.N. Feinberg, A.L. Sanborn, H.E. Kato, K.E. Livingston, T.S. Thorsen, R.C. Kling, S. Granier, P. Gmeiner, S.M. Husbands, J.R. Traynor, W.I. Weis, J. Steyaert, R.O. Dror, B.K. Kobilka, Structural insights into mu-opioid receptor activation, Nature, 524 (2015) 315-+.
41. A. Sali, T.L. Blundell, Comparative protein modelling by satisfaction of spatial restraints, J. Mol. Bio. 234 (1993) 779-815.
42. E.F. Pettersen, T.D. Goddard, C.C. Huang, G.S. Couch, D.M. Greenblatt, E.C. Meng, T.E. Ferrin, UCSF Chimera--a visualization system for exploratory research and analysis, J. Comput. Chem. 25 (2004) 1605-1612.
43. Sybyl-X, version 2.1.1; Tripos, 1991-2012, Certara.
44. D.P. Tieleman, H.J. Berendsen, M.S. Sansom, Surface binding of alamethicin stabilizes its helical structure: molecular dynamics simulations, Biophys. J. 76 (1999) 3186-3191.
45. M. Rarey, B. Kramer, T. Lengauer, G. Klebe, A fast flexible docking method using an incremental construction algorithm, J. Mol. Bio. 261 (1996) 470-489.
46. Dassault Systems BIOVIA, Discovery Studio Modelling Environment, Release 4.1, San Diego; Dassault Systems, 2015.
47. https://www.ebi.ac.uk/thornton-srv/databases/pdbsum/Generate.html
48. S. Tunaru, J. Lattig, J. Kero, G. Krause, S. Offermanns, Characterization of determinants of ligand binding to the nicotinic acid receptor GPR109A (HM74A/PUMA-G), Mol. Pharmac. 68 (2005) 1271-1280.

49. Q. Deng, J.L. Frie, D.M. Marley, R.T. Beresis, N. Ren, T.Q. Cai, A.K. Taggart, K. Cheng, E. Carballo-Jane, J. Wang, X. Tong, M.G. Waters, J.R. Tata, S.L. Colletti, Molecular modeling aided design of nicotinic acid receptor GPR109A agonists, Bioorg. Med. Chem. Lett. 18 (2008) 4963-4967.
50. J.U. Peters, H. Kuhne, H. Dehmlow, U. Grether, A. Conte, D. Hainzl, C. Hertel, N.A. Kratochwil, M. Otteneder, R. Narquizian, C.G. Panousis, F. Ricklin, S. Rover, Pyrido pyrimidinones as selective agonists of the high affinity niacin receptor GPR109A: optimization of in vitro activity, Bioorg. Med. Chem. Lett. 20 (2010) 5426-5430.
51. C. Kopp, S.P. Singh, P. Regenhard, U. Muller, H. Sauerwein, M. Mielenz, Trans-cinnamic acid increases adiponectin and the phosphorylation of AMP-activated protein kinase through G-protein-coupled receptor signaling in 3T3-L1 adipocytes, Inter. J. Mol. Sci. 15 (2014) 2906-2915.
52. J.S. Flier, Clinical review 94: What's in a name? In search of leptin's physiologic role, The J. Clin. Endocrin. Metabol. 83 (1998) 1407-1413.
53. L.A. Carlson, Nicotinic acid: the broad-spectrum lipid drug. A 50th anniversary review, J. Internal Med. 258 (2005) 94-114.

Research highlights:

- Compounds 10c exhibited GPR109a receptor agonist activity (EC_{50} =10.6 nM).
- Chronic treatment with 10c significantly decreased body weight gain in obese mice.
- Treatment of 10c increased leptin sensitivity in obese mice.
- Compounds 10c modestly decreased total cholesterol level in obese mice